et al., 2004; Song *et al.*, 1999). The SNARE-like membrane fusion proteins VAP-A and VAP-B have been reported to interact with NS5A, and the binding capacity is inversely correlated to the degree of NS5A phosphorylation (Evans *et al.*, 2004; Gao *et al.*, 2004; Hamamoto *et al.*, 2005). NS5A binds to and inhibits double-stranded RNA-dependent protein kinase (PKR) (Gale *et al.*, 1998) and 2′,5′-oligoadenylate synthetase (Taguchi *et al.*, 2004). NS5A seems to have the potential to regulate not only interferon responses but also many other cellular functions, such as mitogenic signalling, apoptosis, the cell cycle and reactive oxygen species signalling, by interacting with a variety of host proteins (Macdonald *et al.*, 2004). These NS5A-interacting proteins include SRCAP (Ghosh *et al.*, 2000), Grb2 (He *et al.*, 2002; Tan *et al.*,1999), p53 (Majumder *et al.*, 2001; Qadri *et al.*, 2002), phosphatidylinositol 3-kinase p85 subunit (He *et al.*, 2002; Street *et al.*, 2004), karyopherin β3 (Chung *et al.*, 2000), apolipoprotein A1 (Shi *et al.*, 2002), amphiphysin II (Zech *et al.*, 2003) and Src family protein tyrosine kinases (Macdonald & Harris, 2004; Macdonald *et al.*, 2004).

The non-receptor protein tyrosine kinase Syk is widely expressed in cells of the haematopoietic lineage, endothelium, epithelium and hepatocytes (Coopman *et al.*, 2000; Sada *et al.*, 2001; Tsuchida *et al.*, 2000; Turner *et al.*, 2000; Yanagi *et al.*, 1995, 2001). Syk contains tandem SH2 and kinase domains that are connected by an inter-SH2 domain and a linker region (Taniguchi *et al.*, 1991). The tandem SH2 domains of Syk bind to diphosphorylated immunoreceptor tyrosine-based activation motifs [ITAMs: YXX(L/I)X_{6-8}YXX(L/I)] in the cytoplasmic tail of the Fc receptor γ-chain or B-cell receptor subunit Igα to be activated after the engagement of immune receptors (Kurosaki *et al.*, 1995; Sada *et al.*, 2001; Shiue *et al.*, 1995; Turner *et al.*, 1995; Weiss & Littman, 1994). Autophosphorylation of Syk on Tyr^{525} and Tyr^{526} in the activation loop of the kinase domain results in an increase in its intrinsic kinase activity to phosphorylate its downstream signalling molecules, such as phospholipase C (PLC)-γ (Kurosaki *et al.*, 1995). Autophosphorylation on Tyr^{352} in the linker region is required for tyrosine phosphorylation of PLC-γ1 (Law *et al.*, 1996). Genetic studies have demonstrated that Syk is required for the development and maturation of B cells, mast-cell activation and platelet aggregation (Cheng *et al.*, 1995; Costello *et al.*, 1996; Poole *et al.*, 1997; Turner *et al.*, 1995, 2000). Furthermore, it has been reported that Syk functions as a tumour suppressor in breast cancers and that loss of Syk expression appears to be associated with malignant phenotypes (Coopman *et al.*, 2000).

In the present study, we demonstrated that HCV NS5A interacts physically with Syk to inhibit its kinase activity in human hepatoma-derived Huh-7 cells. Our results indicate that NS5A-induced downregulation of the possible tumour suppressor Syk may play a role in malignant transformation of HCV-infected hepatocytes.

METHODS

Expression plasmids. Mammalian expression plasmids for each of the Myc-tagged HCV proteins were constructed by amplifying and subcloning the corresponding cDNA fragments of pFK5B/2884Gly (Lohmann *et al.*, 2001) in frame to the pEF1/Myc-His(−) vector (Invitrogen). pFK5B/2884Gly was a kind gift from Dr R. Bartenschlager (University of Heidelberg, Germany). An expression plasmid for a polyprotein consisting of NS3–NS5B was amplified from pFK5B/2884Gly and subcloned into pEF1/Myc-His(−). Deletion mutants of NS5A were also amplified by PCR and subcloned into pEF1/Myc-His(−). Point mutations in NS5A [Tyr^{118} to Phe (Y118F), Val^{121} to Ala (V121A)] were introduced into pEF1/NS5A-Myc-His(−) by site-directed mutagenesis. Human Syk cDNA was a gift from Dr B. Müller-Hilke (University of Rostock, Germany). cDNA fragments for FLAG-tagged truncated forms and the kinase-inactive form of Syk were generated by PCR. All mutant forms of FLAG-tagged Syk were subcloned into pcDNA3.1/Hygro(+) (Invitrogen).

Cells, HCV RNA replicon and virus. Huh-7 human hepatoma-derived cells were maintained in Dulbecco's modified Eagle's medium supplemented with 10% heat-inactivated fetal calf serum (FCS). Huh-7.5 cells (Blight *et al.*, 2002) were kindly provided by Dr C. M. Rice (The Rockefeller University, USA). BJAB cells, a human B-cell line expressing endogenous Syk, were cultured in RPMI 1640 supplemented with 10% FCS.

Huh-7.5 cells stably harbouring an HCV subgenomic RNA replicon were prepared by using pFK5B/2884Gly, as described previously (Hidajat *et al.*, 2005; Lohmann *et al.*, 2001; Taguchi *et al.*, 2004; Takigawa *et al.*, 2004).

The plasmid pFL-J6/JFH1 encoding the entire genome of the HCV J6/JFH-1 strain was kindly provided by Dr C. M. Rice, and cell-free virus was propagated in Huh-7.5 cell cultures, as described previously (Lindenbach *et al.*, 2005).

Protein expression. Protein expression was performed using a recombinant vaccinia virus expressing T7 RNA polymerase (vTF7-3), as described previously (Deng *et al.*, 2006; Muramatsu *et al.*, 1997). In some experiments, protein expression was performed using a plasmid-based expression system without vTF7-3. For BJAB cells, we used an electroporation method (Schneider & Kieser, 2004). In brief, 3×10^6 cells were washed once with PBS and incubated for 10 min with 15 μg plasmid DNA in 250 μl RPMI 1640. Electroporation was carried out in a 4 mm cuvette using a Bio-Rad Gene Pulser II with a capacity of 975 μF and a voltage of 180 V. Immediately after electroporation, 500 μl FCS was added to the cells, which were then transferred to 4.5 ml RPMI 1640.

To activate Syk under hyperosmolarity conditions, cells were incubated with serum-free medium containing 400 mM sorbitol for 30 min at 37 °C, as described previously (Miah *et al.*, 2004). In addition, cells were treated with sodium pervanadate (generated by mixing 0.1 mM Na_3VO_4 with 1 mM H_2O_2) for 30 min to activate Syk (Wienands *et al.*, 1996).

Immunohistochemistry. Human normal adult liver autopsy materials and surgically resected liver tissue of patients with HCV-associated HCC were obtained with written informed consent. The tissues were fixed with 10% buffered formalin, embedded in paraffin and sectioned. Immunohistochemical staining was performed with a Dako EnVision+ kit, according to the manufacturer's instructions. In brief, fixed sections were depleted of paraffin by treatment with xylene, dehydrated in ethanol and incubated with 3% H_2O_2 to quench endogenous peroxidase activity. After being autoclaved at 121 °C for 20 min, the sections were incubated with a blocking

solution and then with anti-Syk rabbit polyclonal antibody (N-19; Santa Cruz Biotech). Normal rabbit IgG served as a control. The sections were then incubated with horseradish peroxidase-labelled polymer-conjugated secondary antibody. The sections were counter-stained with haematoxylin and examined under a light microscope. To confirm the specificity of immunostaining, anti-Syk antibody was pre-incubated with a 1000-fold excess of blocking peptide (Santa Cruz Biotech) for 2 h at room temperature prior to staining.

Detection of HCV RNA by *in situ* RT-PCR. *In situ* RT-PCR was performed as described previously (Maeda *et al.*, 2004) with some modifications. Briefly, OCT-embedded frozen liver biopsy sections were fixed with 10 % formaldehyde and treated with proteinase K. The samples were subjected to *in situ* reverse transcription using Moloney murine leukemia virus reverse transcriptase with an antisense primer for HCV (nt 290–272; 5′-AGTACCACAA GGCCTTTCG-3′), followed by *in situ* PCR using an *in situ* PCR System 1000 (Applied Biosystems) in the reaction mixture containing the antisense and a sense primer (nt 129–147; 5′-CCGGGAGAG CCATAGTGGT-3′). After being fixed in 4 % paraformaldehyde, the PCR products were detected by *in situ* hybridization using a digoxigenin (DIG)-labelled oligonucleotide probe, 5′-(DIG)-ATTTGGGCTGTGCCCCCGCGAGACTGCTAGCCGAGTAGTGTT-GGGT-$(DIG)_n$-3′ (nt 225–270). Anti-DIG antibody conjugated with alkaline phosphatase (Roche) was used to detect the probe. The slides were incubated in a dye solution containing nitro blue tetrazolium, 5-bromo-4-chloro-3-indolylphosphate and levamizole to yield a purplish-blue precipitate.

Immunoprecipitation and Western blotting. Cultured cells were lysed with a buffer containing 1 % Triton X-100, 50 mM Tris/HCl (pH 7.4), 150 mM NaCl, 10 mM EDTA, 1 mM NaF, 1 mM Na_3VO_4 and 1 mM PMSF. The lysate was centrifuged at 12 000 *g* for 20 min at 4 °C and the supernatant was immunoprecipitated with appropriate antibodies. In the case of liver tissue, each tissue sample was placed in a tube containing glass beads (1 mm diameter; BioSpec Products) to which 1 ml lysis buffer was added. The tube was then shaken at 4 °C for 3 min using a Mini-BeadBeater (BioSpec Products) to homogenize the tissues. After centrifugation at 80 *g* for 3 min, the supernatant was collected for immunoprecipitation analysis.

Immunoprecipitation and Western blot analyses were performed as described previously (Deng *et al.*, 2006). In brief, the supernatants of the lysates were pre-cleared with control IgG and protein G–Sepharose 4 Fast Flow (GE Healthcare) and incubated with appropriate antibodies at 4 °C for 1 h, followed by incubation with protein G–Sepharose 4 Fast Flow for another 1 h. After six washes with lysis buffer, the immunoprecipitates were analysed by Western blotting.

Antibodies used were as follows: anti-FLAG rabbit polyclonal antibody (Sigma); anti-Myc polyclonal and monoclonal antibodies (Santa Cruz Biotech); anti-Syk monoclonal antibody (4D10; Santa Cruz Biotech); anti-phospho Syk(Tyr^{352}) and Syk($Tyr^{525/526}$) rabbit polyclonal antibodies (Cell Signaling Technology); anti-PLC-γ1 monoclonal antibody (BD Biosciences); mouse monoclonal antibodies against core (Yasui *et al.*, 1998), NS3, NS4A and NS5A (kind gifts from Dr I. Fuke, Osaka University, Japan); anti-NS5A rabbit polyclonal antibody (NS5ACL1; a kind gift from Dr K. Shimotohno, Kyoto University, Japan; Miyanari *et al.*, 2007); and anti-NS5B goat polyclonal antibody (sc-17532; Santa Cruz Biotech). Normal IgG served as a control.

***In vitro* protein kinase assay.** An *in vitro* protein kinase assay was performed as reported previously (Miah *et al.*, 2004; Sada *et al.*, 2000, 2001). In brief, immunoprecipitates obtained with anti-Syk antibody from differentially transfected cells were incubated with 10 μg H2B histone (Sigma) as substrate in 20 μl kinase buffer, composed of 30 mM HEPES (pH 7.5), 10 mM $MgCl_2$, 2 mM $MnCl_2$, 4 μM ATP and 4 μCi (148 kBq) [γ-^{32}P]ATP, for 30 min at room temperature. Reactions were terminated by boiling for 5 min in 2 × sample buffer.

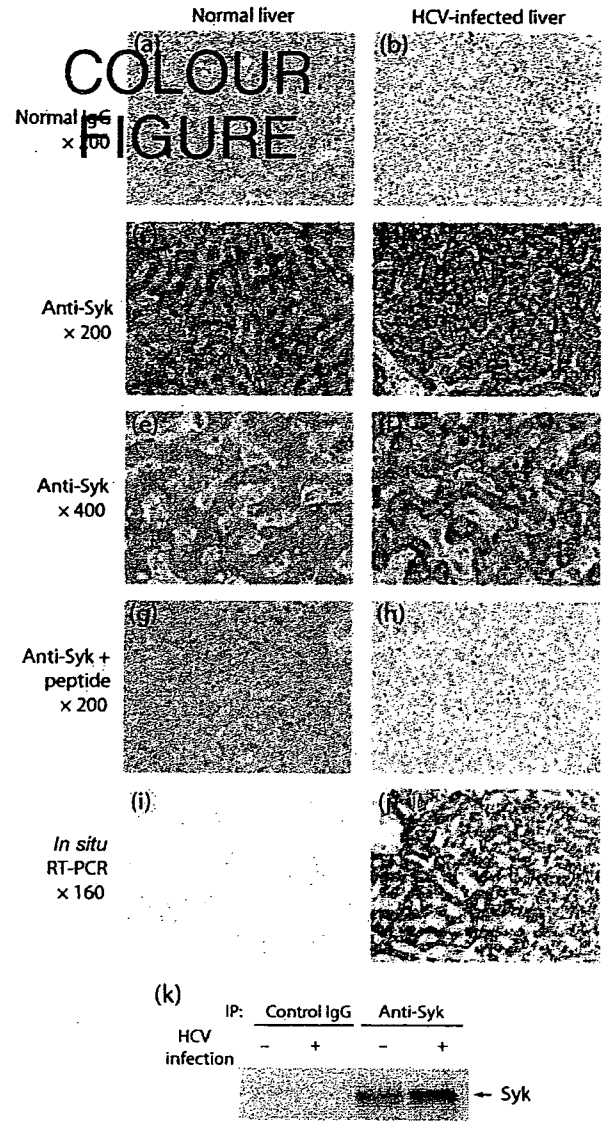

Fig. 1. Endogenous Syk expression in human liver tissues *in vivo*. Normal liver tissues (a, c, e, g, i) and HCV-infected non-cancerous liver tissues (b, d, f, h, j) were analysed. Formalin-fixed samples were stained with control IgG (a, b) or anti-Syk polyclonal antibody without (a–f) or with (g, h) pre-incubation with an excess amount of the immunogenic peptides. Frozen tissues were sectioned and examined for the presence of HCV RNA by *in situ* RT-PCR (i, j). Representative results are shown from four normal livers and ten HCV-infected livers. (k) Western blot analysis of normal human liver and HCV-infected non-cancerous liver. Supernatants of liver tissue homogenates (1.75 mg protein equivalent) were immunoprecipitated with anti-Syk monoclonal antibody (4D10) and probed with the same antibody or with control IgG.

Proteins were separated by SDS-PAGE. The gels were treated with 1 M KOH for 1 h at 56 °C to remove phosphoserine and most of the phosphothreonine. After gel drying, radiolabelled proteins were visualized by autoradiography. For quantitative analysis, γ-^{32}P incorporation was measured using a PhosphorImager (BAS2000; Fuji) and protein amounts with an LAS1000 image analyser (Fuji).

RESULTS

Different expression patterns of endogenous Syk in normal and HCV-infected liver tissues

We first examined whether Syk was expressed in human liver tissues. Immunohistochemical analysis revealed that Syk was indeed expressed and rather diffusely distributed throughout the cytoplasm of normal adult hepatocytes (Fig. 1c, e). This pattern was observed with four out of four normal liver tissues (100%; data not shown). The specificity of the staining was verified by pre-incubating the antibody with an excess amount of the immunogenic peptides (Fig. 1g, h). We then examined Syk expression in non-cancerous liver tissue obtained from patients with HCV-associated HCC. Interestingly, Syk was detected near the plasma membrane with a patchy pattern in hepatocytes of eight out of ten HCV-infected patients (80%; Fig. 1d, f, and data not shown). All of the specimens stained with normal rabbit IgG were negative (Fig. 1a, b). We confirmed that almost all off the hepatocytes in the tissue samples were infected with HCV using *in situ* RT-PCR (Fig. 1i, j).

Western blot analysis confirmed Syk expression in human liver tissue, irrespective of HCV infection (Fig. 1k). It should be noted, however, that the Syk expression was rather weak, as we could achieve successful Western blotting only after the tissue lysates were concentrated by immunoprecipitation with specific antibody. Also, possibly due to the low level of expression and comparatively low sensitivity of the antibodies used for Western blotting, we could not detect the phosphorylated forms of Syk in the liver tissue (data not shown).

Identification of Syk as a novel NS5A-interacting protein

We then examined the possible interaction between HCV proteins and Syk in cultured cells. For this purpose, various HCV proteins and Syk were expressed ectopically in Huh-7 cells, as these cells do not express endogenous Syk. Co-immunoprecipitation analysis revealed that NS5A associated with Syk, whereas the other HCV proteins associated with Syk very weakly or not at all (Fig. 2a, b). A specific interaction of NS5A with Syk was also observed when NS5A was expressed as part of an NS3–NS5B polyprotein (Fig. 2c). These results collectively suggested that NS5A interacts specifically with Syk.

Next, we examined the possible interaction of NS5A with endogenously expressed Syk. As human hepatoma-derived cell lines, such as Huh-7, HepG2 and FLC4, are negative for

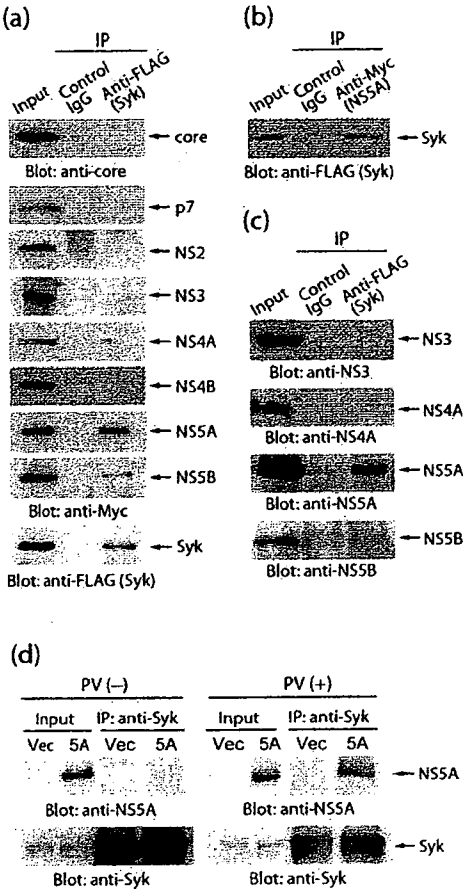

Fig. 2. NS5A specifically interacts with Syk in Huh-7 cells. (a) Each of the Myc-tagged HCV proteins was expressed with FLAG-tagged full-length Syk. Cell lysates were immunoprecipitated using anti-FLAG antibody or control IgG. Cell lysates (input) and the immunoprecipitates were probed with anti-core or anti-Myc antibodies. A representative result verifying efficient immunoprecipitation is shown at the bottom. (b) Myc-tagged NS5A was expressed with FLAG-tagged full-length Syk. Cell lysates were immunoprecipitated using anti-Myc antibody or control IgG, and probed with anti-FLAG antibody. (c) A polyprotein consisting of NS3–NS5B was expressed with FLAG-tagged Syk. Cell lysates were immunoprecipitated with anti-FLAG antibody or control IgG, and probed with the indicated antibodies. (d) NS5A was expressed in BJAB cells expressing endogenous Syk. The cells were treated with pervanadate (PV) or left untreated. Cell lysates were immunoprecipitated with anti-Syk monoclonal antibody and probed with anti-NS5A or anti-Syk monoclonal antibody. Vec, control using empty vector.

endogenous Syk expression, we used BJAB cells endogenously expressing Syk. Unlike ectopically expressed Syk, endogenous Syk in BJAB cells is not tyrosine phosphorylated. Therefore, we treated the cells with pervanadate to induce tyrosine phosphorylation of Syk. Co-immunoprecipitation experiments clearly demonstrated that NS5A

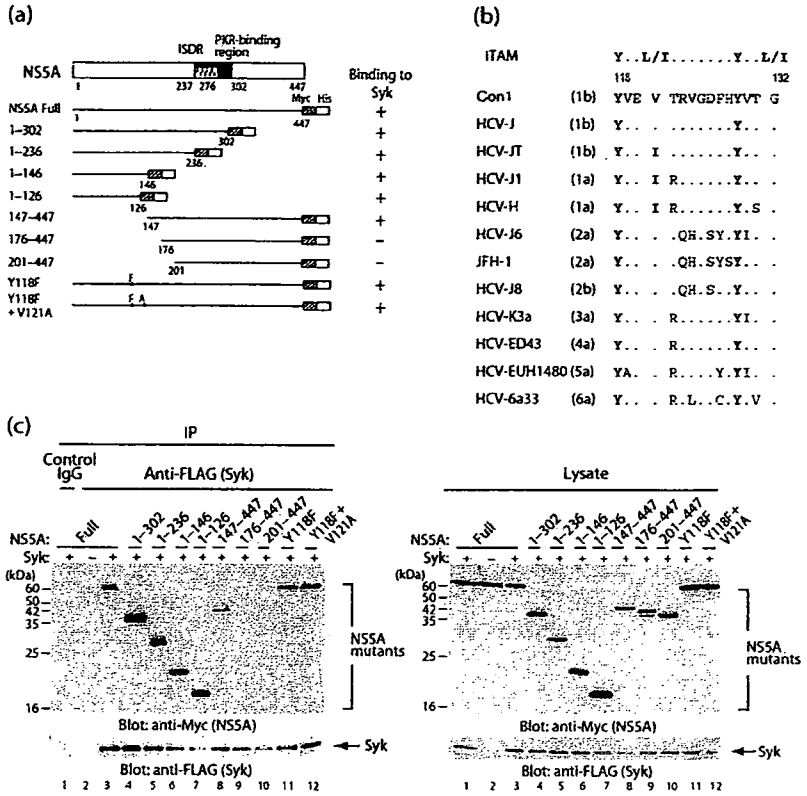

Fig. 3. Determination of the Syk-binding region(s) of NS5A. (a) Schematic diagram of various deletion mutants of NS5A and their Syk-binding capacity. (b) Alignment of amino acid sequences surrounding the ITAM-related sequence in NS5A of various HCV strains. The genotype is indicated in parentheses. Residues identical to those of HCV strain Con1 are shown by a dot. Residues identical to ITAM are shown in bold. (c) Full-length (Full) and a series of deletion mutants of Myc-tagged NS5A were expressed in Huh-7 cells with or without FLAG-tagged full-length Syk. Cell lysates were immunoprecipitated using anti-FLAG antibody and probed with anti-Myc antibody (left panel). Efficient immunoprecipitation was verified (bottom). Cell lysates were probed directly with anti-Myc and anti-FLAG antibodies to verify comparable expression levels of the NS5A mutants and Syk, respectively (right panels).

interacted with endogenous Syk when the cells were treated with pervanadate, but not when the cells were left untreated (Fig. 2d).

The N-terminal region of NS5A is required for interaction with Syk

To map a Syk-interacting region(s) of NS5A, interaction between various deletion mutants of NS5A and Syk was tested. C-terminally deleted mutants of NS5A up to aa 126, as well as the full-length NS5A, were co-immunoprecipitated with Syk (Fig. 3a, c). This result suggested that neither the PKR-binding region nor the interferon sensitivity-determining region (ISDR) of NS5A was required for the interaction with Syk. A proline-rich region of NS5A (aa 343–356), which is reported to bind to the Src family kinases (Macdonald & Harris, 2004; Macdonald *et al.*, 2004), was not involved in the Syk interaction either. In contrast, the N-terminally truncated mutant of NS5A(147–447), but not the further truncated mutants NS5A(176–447) or NS5A(201–447), was co-immunoprecipitated with Syk, suggesting that a region of NS5A between aa 147 and 175 is also involved in the interaction with Syk. We also observed that NS5A(1–126) and NS5A(174–447), but not NS5A(201–447), interacted with Syk(1–261) or Syk(379–635) (data not shown). These results collectively suggested that NS5A interacts with Syk through two independent regions of NS5A (aa 1–126 and 147–175).

Syk is activated by interaction with a diphosphorylated ITAM of immune receptors (Sada *et al.*, 2001; Turner *et al.*, 2000; Weiss & Littman, 1994). NS5A from HCV strain Con1 possesses a sequence (AEEY^{118}VEV^{121}-TRVGDFHY^{129}VTG) that resembles an ITAM (Fig. 3b). We found that the two tyrosine residues at positions 118 and 129 are highly conserved across different genotypes and subtypes. The tyrosine at position 118 is exposed on

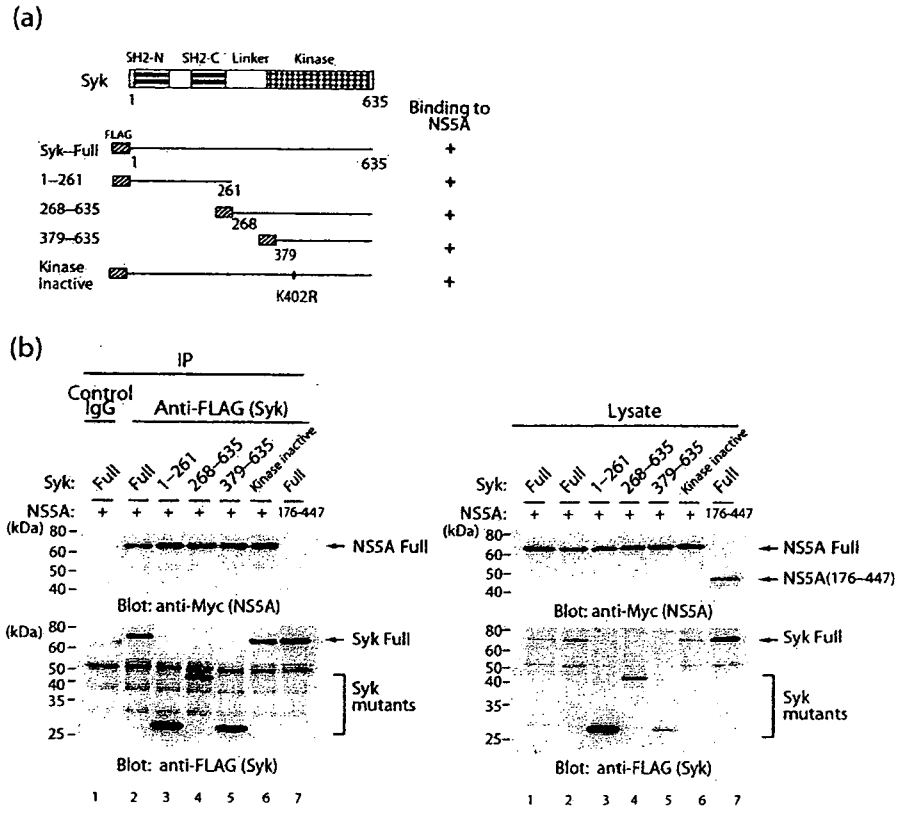

Fig. 4. NS5A interacts with both N-terminal and C-terminal regions of Syk. (a) Schematic diagram of the deletion mutants of Syk and their NS5A-binding capacity. (b) Full-length (Full) and a series of domain-deletion mutants of FLAG-tagged Syk was expressed in Huh-7 cells with Myc-tagged full-length NS5A (lanes 1–6) or NS5A(176–447) (lane 7). Cell lysates were immunoprecipitated using anti-FLAG antibody and probed with anti-Myc antibody (left upper panel). Efficient immunoprecipitation of Syk deletion mutants was verified (bottom). Cell lysates were probed directly with anti-Myc and anti-FLAG antibodies to verify comparable expression levels of the NS5A and Syk mutants, respectively (right panels).

the surface of the NS5A molecule (Tellinghuisen *et al.*, 2005). We examined whether this sequence motif was involved in the interaction with Syk. A single point mutation of Tyr^{118} (Y118F) or double mutations of Tyr^{118} and Val^{121} (Y118F and V121A) in NS5A did not affect the interaction with Syk (Fig. 3c, lanes 11 and 12). Thus, it is unlikely that NS5A binds to Syk through its ITAM-related sequence in the same manner as that observed for immune receptors.

To map the NS5A-binding region in Syk, a series of domain-deleted mutants of Syk was examined. The results obtained revealed that both N-terminal (tandem SH2 domains) and C-terminal halves (linker and the kinase domain) interacted with NS5A (Fig. 4). The kinase domain alone and a kinase-inactive form of Syk were also co-immunoprecipitated with NS5A. These results suggested that the NS5A–Syk interaction occurs through the N- and C-terminal regions of Syk and that the catalytic activity of Syk is not necessary for the interaction.

NS5A expression downregulates the kinase activity of Syk

Next, we tested the possible effect of NS5A expression on Syk kinase activity. An *in vitro* kinase assay revealed that full-length NS5A and a C-terminally deleted NS5A(1–302) mutant significantly inhibited Syk kinase activity (Fig. 5, lanes 2–4). In contrast, NS5A(1–236), which lacked both the PKR-binding region (aa 237–302) and ISDR (aa 237–276), failed to inhibit Syk kinase activity, although it could interact with Syk. NS5A(176–447), which contained the PKR-binding region and ISDR but lacked the Syk-binding region, did not affect Syk kinase activity. These results collectively suggested that NS5A requires both N-terminal (aa 1–175) and central (aa 237–302) regions for the downregulation of Syk kinase activity (Table 1).

To address the relevance of the interaction between NS5A and Syk, the possible effect(s) of NS5A on Syk-mediated cellular signalling in Huh-7 cells was examined. Ectopic

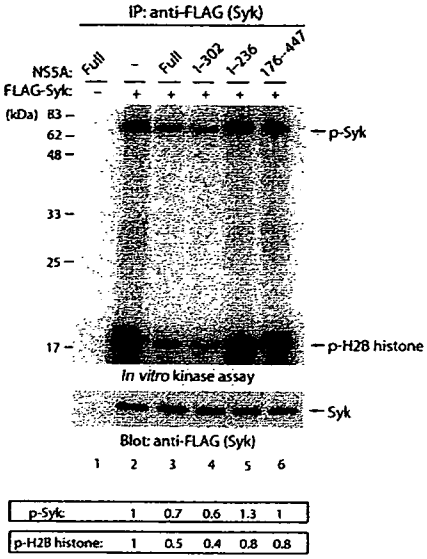

Fig. 5. NS5A downregulates Syk kinase activity. Myc-tagged NS5A and FLAG-tagged Syk were expressed in Huh-7 cells. Cell lysates were immunoprecipitated with anti-FLAG antibody and the immunoprecipitates were subjected to an *in vitro* kinase assay using H2B histone as substrate. Phosphorylation of Syk (p-Syk) and H2B histone (p-H2B histone) was visualized by autoradiography (upper panel). Efficient immunoprecipitation of Syk was verified (lower panel). Arbitrary units of Syk kinase activities, represented by the phosphorylation values of p-Syk and p-H2B histone normalized to the amounts of immunoprecipitated Syk, are shown at the bottom.

expression of Syk alone mediated signal transduction to induce tyrosine phosphorylation of a wide variety of cellular proteins, either directly or indirectly (Fig. 6a, lanes 1 and 3). Hyperosmolarity stress (400 mM sorbitol treatment) enhanced Syk-mediated tyrosine phosphorylation of cellular proteins (Fig. 6a, lanes 3 and 4), with the result being consistent with the previous observation (Miah *et al.*, 2004). Interestingly, co-expression of NS5A decreased Syk-mediated tyrosine phosphorylation of cellular proteins both in the absence and presence of hyperosmolarity stress (Fig. 6a, lanes 7 and 8). The phosphorylation of Syk on Tyr^{352} and/or $Tyr^{525/526}$ is a marker for Syk activation. Using these parameters, we confirmed that co-expression of NS5A inhibited Syk activation both in the absence and presence of hyperosmolarity stress (Fig. 6b).

PLC-γ1 has been reported to be a downstream molecule of Syk-mediated signal transduction (Law *et al.*, 1996). Our results demonstrated that NS5A inhibited PLC-γ1 phosphorylation, probably through downregulation of Syk kinase activity, both in the absence and presence of hyperosmolarity stress (Fig. 6c).

Table 1. Summary of NS5A deletion mutational analysis of the interaction with Syk and inhibition of Syk kinase activity

NS5A mutant	Interaction with Syk	Inhibition of Syk
NS5A(1–447; full)	+	+
NS5A(1–302)	+	+
NS5A(1–236)	+	–
NS5A(176–447)	–	–

NS5A expressed in the context of HCV RNA replication interacts with Syk in Huh-7.5 cells

The interaction of NS5A with Syk was examined further using Huh-7.5 cells harbouring an HCV subgenomic RNA replicon. The results obtained clearly demonstrated that NS5A expressed in the context of HCV RNA replication interacted with Syk (Fig. 7a). It is well known that NS5A takes two forms, p56 and p58, with the former being the basally phosphorylated form and the latter the hyperphosphorylated form (Kaneko *et al.*, 1994; Song *et al.*, 1999). It is noteworthy that Syk interacted with p56 more efficiently than with p58.

We also examined the interaction of NS5A with Syk in Huh-7.5 cells infected with the J6/JFH-1 strain of HCV. The results demonstrated that NS5A interacted with Syk in HCV-infected cells (Fig. 7b). These results collectively suggested that the NS5A–Syk interaction occurs in the context of virus replication, where NS5A is primarily utilized to form the viral replication complex. In this connection, HCV J6/JFH-1 replication was not affected significantly by ectopically expressed Syk in Huh-7.5 cells (data not shown). This observation, however, does not necessarily exclude the possibility that the NS5A interaction with Syk exerts certain biological effect(s) on the host cell's fate.

Syk kinase activity is suppressed in the context of HCV RNA replication

We then examined Syk kinase activity in the HCV subgenomic RNA-harbouring Huh-7.5 cells. An *in vitro* kinase assay demonstrated that Syk kinase activities, represented by autophosphorylation of Syk (p-Syk) and phosphorylation of a substrate (p-H2B histone), were significantly suppressed in HCV RNA-replicating cells compared with the control (Fig. 7c). These results suggested the possibility that Syk kinase activity is downregulated through an NS5A–Syk interaction in HCV-infected hepatocytes as well.

DISCUSSION

The non-receptor protein tyrosine kinase Syk is expressed in a wide variety of haematopoietic cell lineages (Taniguchi *et al.*, 1991). It is also expressed in human mammary

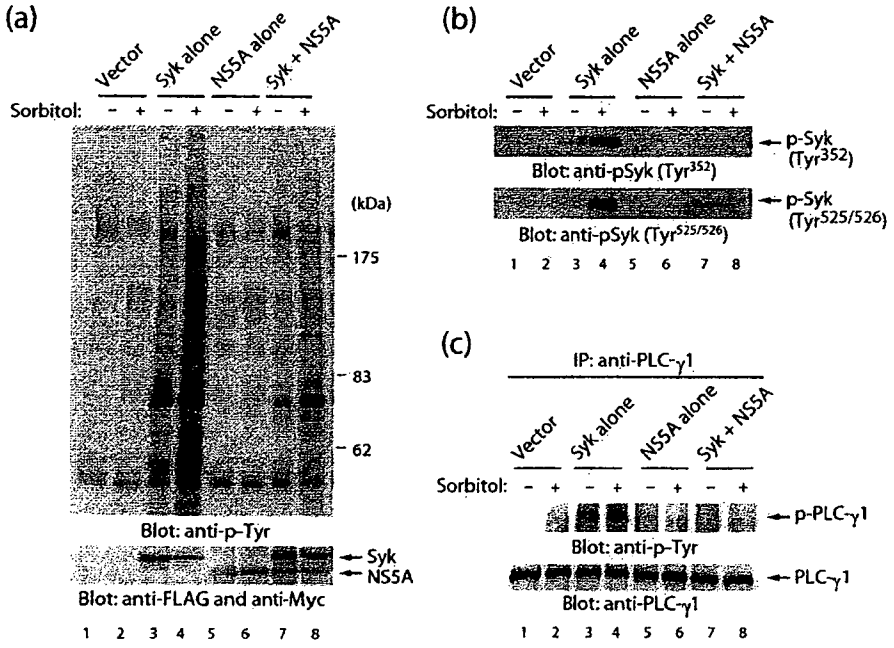

Fig. 6. NS5A suppresses hyperosmolarity stress-induced Syk-mediated tyrosine phosphorylation of cellular proteins. (a) Myc-tagged NS5A was expressed in Huh-7 cells with or without FLAG-tagged Syk. The cells were incubated with or without 400 mM sorbitol for 30 min and then lysed in lysis buffer. Half of the cell lysate was probed with anti-phosphotyrosine (p-Tyr) antibody (upper panel) and the remaining half with anti-FLAG and anti-Myc antibodies (bottom). (b) Cell lysates were probed with anti-p-Syk(Tyr^{352}) (upper panel) or anti-p-Syk($Tyr^{525/526}$) antibody (lower panel). (c) Cell lysates were immunoprecipitated using anti-PLC-γ1 antibody and probed with anti-p-Tyr antibody (upper panel). Efficient immunoprecipitation of PLC-γ1 was verified (lower panel).

(Coopman *et al.*, 2000) and airway epithelial cells (Ulanova *et al.*, 2005), nasal fibroblasts (Yamada *et al.*, 2001) and hepatocytes (Tsuchida *et al.*, 2000). These results suggest that Syk plays a general physiological role in non-haematopoietic cells as well. The first report of Syk having a role in cancer was a study of mammary epithelial cells (Coopman *et al.*, 2000). Since then, there have been several reports that Syk functions as a tumour suppressor in the process of malignant tumour development, such as gastric cancer (Wang *et al.*, 2004) and leukaemia (Goodman *et al.*, 2001). To look into the possible relevance of Syk in HCV-infected hepatocytes and also the possible involvement of Syk in HCC development, we first examined Syk expression in hepatocytes obtained from HCV-infected and uninfected subjects. We found that Syk was expressed near the plasma membrane of hepatocytes of HCV-infected patients, with a patchy pattern, whereas it was expressed rather diffusely in the cytoplasm of normal, uninfected hepatocytes (Fig. 1).

We also demonstrated that NS5A interacted with Syk and inhibited its kinase activity when expressed ectopically in Huh-7 cells (Figs 2, 5 and 6). The NS5A interaction with Syk was observed even in the context of HCV RNA replication (Fig. 7a, b) and Syk kinase activity was inhibited in HCV RNA replicon-harbouring cells (Fig. 7c). It is likely, therefore, that Syk is a binding partner of NS5A and is functionally inhibited in HCV-infected hepatocytes as well. Whilst an N-terminal portion of NS5A (aa 1–175) was responsible for the binding to Syk, a central portion (aa 237–302) was also required for the inhibition of Syk kinase activity (Figs 3 and 5). It has been reported that NS5A associates with the non-receptor protein tyrosine kinases Lyn and Fyn, members of the Src family kinases, through the proline-rich region of NS5A (aa 343–356) and the SH3 domain of the kinases, thereby inhibiting and activating the kinase activities of Lyn and Fyn, respectively (Macdonald & Harris, 2004; Macdonald *et al.*, 2004). In contrast, Syk does not possess an SH3 domain but has two tandem SH2 domains. These SH2 domains are known to interact with diphosphorylated ITAM of immune receptors, resulting in activation of Syk in an autocrine or paracrine manner (Sada *et al.*, 2001; Yanagi *et al.*, 1995). However, it is unlikely that the NS5A–Syk interaction occurs through its ITAM-related sequence in the same manner as that observed for immune receptors, as NS5A mutants with a mutated ITAM-like sequence still interacted with Syk (Fig. 3). Also, the SH2 domains of Syk are not the only binding sites for NS5A (Fig. 4). These results suggest that the mechanism

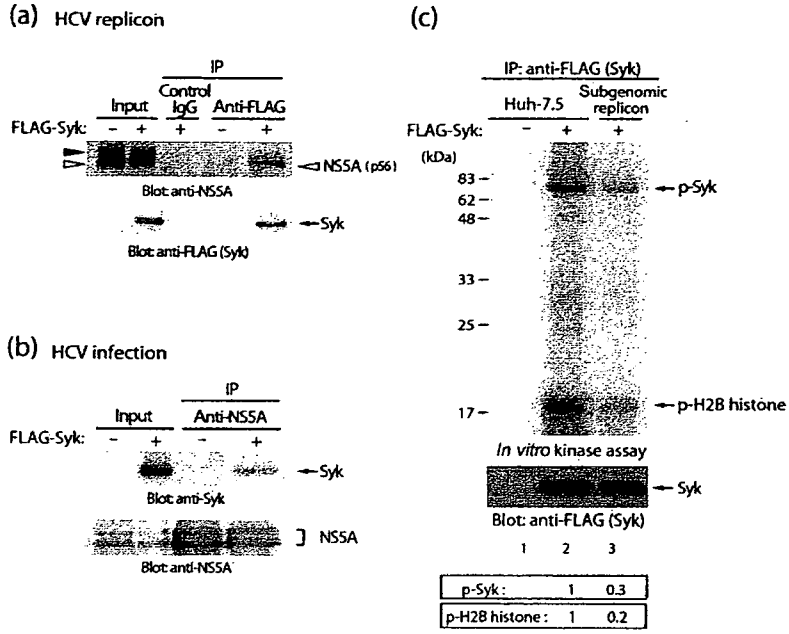

Fig. 7. NS5A expressed in the context of HCV RNA replication interacts with Syk and inhibits its kinase activity. (a) FLAG-tagged Syk was expressed in HCV RNA replicon-harbouring Huh-7.5 cells. Cell lysates were immunoprecipitated with anti-FLAG antibody or control IgG and probed with anti-NS5A (upper panel) or anti-FLAG antibody (lower panel). Filled and open arrowheads indicate the hyperphosphorylated (p58) and hypophosphorylated forms of NS5A (p56), respectively. (b) FLAG-tagged Syk was expressed in HCV J6/JFH-1-infected Huh-7.5 cells. Cell lysates were immunoprecipitated with anti-NS5A polyclonal antibody and probed with anti-Syk monoclonal antibody. (c) FLAG-tagged Syk was expressed in HCV RNA replicon-harbouring Huh-7.5 cells. Cell lysates were immunoprecipitated with anti-FLAG antibody and the immunoprecipitates were subjected to an *in vitro* kinase assay using H2B histone as substrate. Phosphorylation of Syk (p-Syk) and H2B histone (p-H2B histone) was visualized by autoradiography (upper panel). Efficient immunoprecipitation of Syk was verified (lower panel). Arbitrary units of Syk kinase activities, represented by the phosphorylation values of p-Syk and p-H2B histone normalized to the amounts of immunoprecipitated Syk, are shown at the bottom.

underlying the NS5A–Syk interaction differs from what has been observed for Syk and its interacting proteins in immune cells. It is possible that multiple regions of NS5A are involved in the interaction with Syk. Alternatively, NS5A may interact with Syk indirectly through the other host protein(s) that binds directly to Syk.

Syk is activated by cytokine stimulation, hyperosmolarity shock, oxidative stress and engagement with integrin (Corey *et al.*, 1994; Gao *et al.*, 1997; Miah *et al.*, 2004). However, the biological relevance of Syk in hepatocytes has not yet been demonstrated. We have shown in the present study that hyperosmolarity stress-induced activation of Syk resulted in increased tyrosine phosphorylation of endogenous PLC-γ1 (Fig. 6c). This result suggests that activated Syk sends signals to PLC-γ1 in hepatocytes, as observed in immune cells (Law *et al.*, 1996). Our findings that NS5A associates with Syk strongly suggest that NS5A affects the Syk signalosome to alter the signal transduction elicited by the Syk–PLC-γ1 interaction.

Phosphorylation of tyrosine residues in the linker region of Syk is required for immune receptor signalling. Genetic studies have demonstrated that phosphorylation of Tyr^{348} and Tyr^{352} in the linker region of Syk is involved in regulating tyrosine phosphorylation of LAT (linker for activating T cells), SLP-76 and PLC-γ1 and -γ2, and affects Ca^{2+} mobilization triggered by aggregation of the high-affinity IgE receptor (Simon *et al.*, 2005; Zhang *et al.*, 2002). We observed that NS5A downregulated phosphorylation of Tyr^{352} of Syk (Fig. 6b), which correlated with the inhibition of Syk kinase activity. The phosphorylation state of Tyr^{352} also correlated well with the tyrosine phosphorylation state of PLC-γ1. This suggests the possibility that Ca^{2+} mobilization is affected in HCV-infected hepatocytes through the NS5A-mediated downregulation of Tyr^{352} phosphorylation on Syk.

Unlike ectopically expressed Syk, endogenously expressed Syk in B cells under normal conditions is not tyrosine phosphorylated (Wienands *et al.*, 1996). Pervanadate stimulation is known to induce tyrosine phosphorylation of endogenous Syk. We examined the possible interaction of endogenous Syk and NS5A. Our results demonstrated that NS5A interacted with endogenous Syk when the cells were treated with pervanadate, but not when the cells were left untreated (Fig. 2d). These results suggest that NS5A interacts with the tyrosine-phosphorylated, active form of Syk.

Whilst Syk is commonly expressed in normal human breast tissues, benign breast lesions and low-tumorigenic breast

cancer cell lines, only a minimal or even an undetectable level of Syk expression has been demonstrated in invasive breast carcinoma tissues and cell lines (Coopman *et al.*, 2000). DNA methylation of the CpG sites in the *syk* gene promoter has been reported to be responsible for the loss or marked reduction of Syk expression in breast cancer (Yuan *et al.*, 2001). Moreover, Yuan *et al.* (2006) reported that DNA methylation of the *syk* gene in hepatitis B virus-associated HCC cancerous tissue was highly correlated with Syk expression and that the patients with a methylated *syk* gene had a significantly lower overall survival rate after hepatectomy than those with an unmethylated *syk* gene. In contrast, our results revealed that the expression levels of Syk did not differ between normal and HCV-infected hepatocytes (Fig. 1k) or between cancerous and non-cancerous hepatocytes (data not shown). At the functional level, however, NS5A downregulated Syk kinase activity in Huh-7 cells (Fig. 6). Moreover, Syk kinase activity was downregulated in cells harbouring an HCV RNA replicon (Fig. 7c). These results collectively suggest that NS5A is involved, at least partly, in the suppression of Syk kinase activity in HCV-infected cells. It is also interesting to assume that the NS5A-mediated Syk inhibition plays an important role in the development of HCC, although the precise molecular mechanism(s) is yet to be determined. Recently, a possible mechanism by which breast cancer cells become invasive was proposed: human breast cancer cells express and secrete a group of chemokines called growth-related oncogene (GRO)-α, GRO-β and GRO-γ, and their production is regulated by Syk (Li & Sidell, 2005). It would be interesting to examine the possible effects of NS5A and HCV RNA replication on the levels of GRO expression and secretion.

ACKNOWLEDGEMENTS

The authors are grateful to Dr R. Bartenschlager (University of Heidelberg, Germany) for providing the HCV RNA replicon and Dr C. M. Rice (The Rockefeller University, USA) for pFL-J6/JFH1 and Huh-7.5 cells. Thanks are also due to Dr I. Fuke (Osaka University, Japan) for providing monoclonal antibodies against NS3, NS4A and NS5A, and Dr K. Shimotohno (Institute for Virus Research, Kyoto University, Japan) for anti-NS5A polyclonal antibody. This work was supported in part by Grants-in-Aid for Scientific Research from the Ministry of Education, Culture, Sports, Science and Technology (MEXT) and the Ministry of Health, Labour and Welfare, Japan. This study was also carried out as part of the Program of Founding Research Centers for Emerging and Reemerging Infectious Diseases, MEXT Japan, and the 21st Century COE Program at Kobe University Graduate School of Medicine.

REFERENCES

Blight, K. J., McKeating, J. A. & Rice, C. M. (2002). Highly permissive cell lines for subgenomic and genomic hepatitis C virus RNA replication. *J Virol* 76, 13001–13014.

Cheng, A. M., Rowley, B., Pao, W., Hayday, A., Bolen, J. B. & Pawson, T. (1995). Syk tyrosine kinase required for mouse viability and B-cell development. *Nature* 378, 303–306.

Choo, Q. L., Kuo, G., Weiner, A. J., Overby, L. R., Bradley, D. W. & Houghton, M. (1989). Isolation of a cDNA clone derived from a blood-borne non-A, non-B viral hepatitis genome. *Science* 244, 359–362.

Chung, K. M., Lee, J., Kim, J. E., Song, O. K., Cho, S., Lim, J., Seedorf, M., Hahm, B. & Jang, S. K. (2000). Nonstructural protein 5A of hepatitis C virus inhibits the function of karyopherin β3. *J Virol* 74, 5233–5241.

Coopman, P. J., Do, M. T., Barth, M., Bowden, E. T., Hayes, A. J., Basyuk, E., Blancato, J. K., Vezza, P. R., McLeskey, S. W. & other authors (2000). The Syk tyrosine kinase suppresses malignant growth of human breast cancer cells. *Nature* 406, 742–747.

Corey, S. J., Burkhardt, A. L., Bolen, J. B., Geahlen, R. L., Tkatch, L. S. & Tweardy, D. J. (1994). Granulocyte colony-stimulating factor receptor signaling involves the formation of a three-component complex with Lyn and Syk protein-tyrosine kinases. *Proc Natl Acad Sci U S A* 91, 4683–4687.

Costello, P. S., Turner, M., Walters, A. E., Cunningham, C. N., Bauer, P. H., Downward, J. & Tybulewicz, V. L. (1996). Critical role for the tyrosine kinase Syk in signalling through the high affinity IgE receptor of mast cells. *Oncogene* 13, 2595–2605.

Deng, L., Nagano-Fujii, M., Tanaka, M., Nomura-Takigawa, Y., Ikeda, M., Kato, N., Sada, K. & Hotta, H. (2006). NS3 protein of hepatitis C virus associates with the tumor suppressor p53 and inhibits its function in an NS3 sequence-dependent manner. *J Gen Virol* 87, 1703–1713.

Doi, H., Apichartpiyakul, C., Ohba, K. I., Mizokami, M. & Hotta, H. (1996). Hepatitis C virus (HCV) subtype prevalence in Chiang Mai, Thailand, and identification of novel subtypes of HCV major type 6. *J Clin Microbiol* 34, 569–574.

Evans, M. J., Rice, C. M. & Goff, S. P. (2004). Phosphorylation of hepatitis C virus nonstructural protein 5A modulates its protein interactions and viral RNA replication. *Proc Natl Acad Sci U S A* 101, 13038–13043.

Gale, M., Jr, Blakely, C. M., Kwieciszewski, B., Tan, S. L., Dossett, M., Tang, N. M., Korth, M. J., Polyak, S. J., Gretch, D. R. & Katze, M. G. (1998). Control of PKR protein kinase by hepatitis C virus nonstructural 5A protein: molecular mechanisms of kinase regulation. *Mol Cell Biol* 18, 5208–5218.

Gao, J., Zoller, K. E., Ginsberg, M. H., Brugge, J. S. & Shattil, S. J. (1997). Regulation of the pp72^{syk} protein tyrosine kinase by platelet integrin $\alpha_{IIb}\beta_3$. *EMBO J* 16, 6414–6425.

Gao, L., Aizaki, H., He, J. W. & Lai, M. M. (2004). Interactions between viral nonstructural proteins and host protein hVAP-33 mediate the formation of hepatitis C virus RNA replication complex on lipid raft. *J Virol* 78, 3480–3488.

Ghosh, A. K., Majumder, M., Steele, R., Yaciuk, P., Chrivia, J., Ray, R. & Ray, R. B. (2000). Hepatitis C virus NS5A protein modulates transcription through a novel cellular transcription factor SRCAP. *J Biol Chem* 275, 7184–7188.

Goodman, P. A., Wood, C. M., Vassilev, A., Mao, C. & Uckun, F. M. (2001). Spleen tyrosine kinase (Syk) deficiency in childhood pro-B cell acute lymphoblastic leukemia. *Oncogene* 20, 3969–3978.

Hamamoto, I., Nishimura, Y., Okamoto, T., Aizaki, H., Liu, M., Mori, M., Abe, T., Suzuki, T., Lai, M. M. C. & other authors (2005). Human VAP-B is involved in hepatitis C virus replication through interaction with NS5A and NS5B. *J Virol* 79, 13473–13482.

He, Y., Nakao, H., Tan, S. L., Polyak, S. J., Neddermann, P., Vijaysri, S., Jacobs, B. L. & Katze, M. G. (2002). Subversion of cell signaling pathways by hepatitis C virus nonstructural 5A protein via interaction with Grb2 and P85 phosphatidylinositol 3-kinase. *J Virol* 76, 9207–9217.

Hidajat, R., Nagano-Fujii, M., Deng, L., Tanaka, M., Takigawa, Y., Kitazawa, S. & Hotta, H. (2005). Hepatitis C virus NS3 protein interacts with ELKS-δ and ELKS-α, members of a novel protein family involved in intracellular transport and secretory pathways. *J Gen Virol* **86**, 2197–2208.

Kaneko, T., Tanji, Y., Satoh, S., Hijikata, M., Asabe, S., Kimura, K. & Shimotohno, K. (1994). Production of two phosphoproteins from the NS5A region of the hepatitis C viral genome. *Biochem Biophys Res Commun* **205**, 320–326.

Kurosaki, T., Johnson, S. A., Pao, L., Sada, K., Yamamura, H. & Cambier, J. C. (1995). Role of the Syk autophosphorylation site and SH2 domains in B cell antigen receptor signaling. *J Exp Med* **182**, 1815–1823.

Law, C. L., Chandran, K. A., Sidorenko, S. P. & Clark, E. A. (1996). Phospholipase C-γ1 interacts with conserved phosphotyrosyl residues in the linker region of Syk and is a substrate for Syk. *Mol Cell Biol* **16**, 1305–1315.

Li, J. & Sidell, N. (2005). Growth-related oncogene produced in human breast cancer cells and regulated by Syk protein-tyrosine kinase. *Int J Cancer* **117**, 14–20.

Lindenbach, B. D., Evans, M. J., Syder, A. J., Wolk, B., Tellinghuisen, T. L., Liu, C. C., Maruyama, T., Hynes, R. O., Burton, D. R. & other authors (2005). Complete replication of hepatitis C virus in cell culture. *Science* **309**, 623–626.

Lohmann, V., Korner, F., Dobierzewska, A. & Bartenschlager, R. (2001). Mutations in hepatitis C virus RNAs conferring cell culture adaptation. *J Virol* **75**, 1437–1449.

Macdonald, A. & Harris, M. (2004). Hepatitis C virus NS5A: tales of a promiscuous protein. *J Gen Virol* **85**, 2485–2502.

Macdonald, A., Crowder, K., Street, A., McCormick, C. & Harris, M. (2004). The hepatitis C virus NS5A protein binds to members of the Src family of tyrosine kinases and regulates kinase activity. *J Gen Virol* **85**, 721–729.

Maeda, N., Watanabe, M., Okamoto, S., Kanai, T., Yamada, T., Hata, J., Hozumi, N., Katsume, A., Nuriya, H. & other authors (2004). Hepatitis C virus infection in human liver tissue engrafted in mice with an infectious molecular clone. *Liver Int* **24**, 259–267.

Majumder, M., Ghosh, A. K., Steele, R., Ray, R. & Ray, R. B. (2001). Hepatitis C virus NS5A physically associates with p53 and regulates p21/waf1 gene expression in a p53-dependent manner. *J Virol* **75**, 1401–1407.

Mellor, J., Holmes, E. C., Jarvis, L. M., Yap, P. L. & Simmonds, P. (1995). Investigation of the pattern of hepatitis C virus sequence diversity in different geographical regions: implications for virus classification. *J Gen Virol* **76**, 2493–2507.

Miah, S. M., Sada, K., Tuazon, P. T., Ling, J., Maeno, K., Kyo, S., Qu, X., Tohyama, Y., Traugh, J. A. & Yamamura, H. (2004). Activation of Syk protein tyrosine kinase in response to osmotic stress requires the interaction with p21-activated protein kinase Pak2/γ-PAK. *Mol Cell Biol* **24**, 71–83.

Miyanari, Y., Atsuzawa, K., Usuda, N., Watashi, K., Hishiki, T., Zayas, M., Bartenschlager, R., Wakita, T., Hijikata, M. & Shimotohno, K. (2007). The lipid droplet is an important organelle for hepatitis C virus production. *Nat Cell Biol* **9**, 1089–1097.

Muramatsu, S., Ishido, S., Fujita, T., Itoh, M. & Hotta, H. (1997). Nuclear localization of the NS3 protein of hepatitis C virus and factors affecting the localization. *J Virol* **71**, 4954–4961.

Okamoto, K., Moriishi, K., Miyamura, T. & Matsuura, Y. (2004). Intramembrane proteolysis and endoplasmic reticulum retention of hepatitis C virus core protein. *J Virol* **78**, 6370–6380.

Poole, A., Gibbins, J. M., Turner, M., van Vugt, M. J., van de Winkel, J. G., Saito, T., Tybulewicz, V. L. & Watson, S. P. (1997). The Fc receptor γ-chain and the tyrosine kinase Syk are essential for activation of mouse platelets by collagen. *EMBO J* **16**, 2333–2341.

Qadri, I., Iwahashi, M. & Simon, F. (2002). Hepatitis C virus NS5A protein binds TBP and p53, inhibiting their DNA binding and p53 interactions with TBP and ERCC3. *Biochim Biophys Acta* **1592**, 193–204.

Reed, K. E. & Rice, C. M. (2000). Overview of hepatitis C virus genome structure, polyprotein processing, and protein properties. *Curr Top Microbiol Immunol* **242**, 55–84.

Robertson, B., Myers, G., Howard, C., Brettin, T., Bukh, J., Gaschen, B., Gojobori, T., Maertens, G., Mizokami, M. & other authors (1998). Classification, nomenclature, and database development for hepatitis C virus (HCV) and related virus: proposals for standardization. *Arch Virol* **143**, 2493–2503.

Sada, K., Zhang, J. & Siraganian, R. P. (2000). Point mutation of a tyrosine in the linker region of Syk results in a gain of function. *J Immunol* **164**, 338–344.

Sada, K., Takano, T., Yanagi, S. & Yamamura, H. (2001). Structure and function of Syk protein-tyrosine kinase. *J Biochem* **130**, 177–186.

Schneider, F. & Kieser, A. (2004). A novel assay to quantify cell death after transient expression of apoptotic genes in B- and T-lymphocytes. *J Immunol Methods* **292**, 165–174.

Shi, S. T., Polyak, S. J., Tu, H., Taylor, D. R., Gretch, D. R. & Lai, M. M. (2002). Hepatitis C virus NS5A colocalizes with the core protein on lipid droplets and interacts with apolipoproteins. *Virology* **292**, 198–210.

Shiue, L., Green, J., Green, O. M., Karas, J. L., Morgenstern, J. P., Ram, M. K., Taylor, M. K., Zoller, M. J., Zydowsky, L. D. & other authors (1995). Interaction of $p72^{syk}$ with the γ and β subunits of the high-affinity receptor for immunoglobulin E, FcεRI. *Mol Cell Biol* **15**, 272–281.

Simon, M., Vanes, L., Geahlen, R. L. & Tybulewicz, V. L. (2005). Distinct roles for the linker region tyrosines of Syk in FcεRI signaling in primary mast cells. *J Biol Chem* **280**, 4510–4517.

Song, J., Fujii, M., Wang, F., Itoh, M. & Hotta, H. (1999). The NS5A protein of hepatitis C virus partially inhibits the antiviral activity of interferon. *J Gen Virol* **80**, 879–886.

Street, A., Macdonald, A., Crowder, K. & Harris, M. (2004). The hepatitis C virus NS5A protein activates a phosphoinositide 3-kinase-dependent survival signaling cascade. *J Biol Chem* **279**, 12232–12241.

Taguchi, T., Nagano-Fujii, M., Akutsu, M., Kadoya, H., Ohgimoto, S., Ishido, S. & Hotta, H. (2004). Hepatitis C virus NS5A protein interacts with 2′,5′-oligoadenylate synthetase and inhibits antiviral activity of IFN in an IFN sensitivity-determining region-independent manner. *J Gen Virol* **85**, 959–969.

Takigawa, Y., Nagano-Fujii, M., Deng, L., Hidajat, R., Tanaka, M., Mizuta, H. & Hotta, H. (2004). Suppression of hepatitis C virus replicon by RNA interference directed against the NS3 and NS5B regions of the viral genome. *Microbiol Immunol* **48**, 591–598.

Tan, S. L., Nakao, H., He, Y., Vijaysri, S., Neddermann, P., Jacobs, B. L., Mayer, B. J. & Katze, M. G. (1999). NS5A, a nonstructural protein of hepatitis C virus, binds growth factor receptor-bound protein 2 adaptor protein in a Src homology 3 domain/ligand-dependent manner and perturbs mitogenic signaling. *Proc Natl Acad Sci U S A* **96**, 5533–5538.

Taniguchi, T., Kobayashi, T., Kondo, J., Takahashi, K., Nakamura, H., Suzuki, J., Nagai, K., Yamada, T., Nakamura, S. & Yamamura, H. (1991). Molecular cloning of a porcine gene *syk* that encodes a 72-kDa protein-tyrosine kinase showing high susceptibility to proteolysis. *J Biol Chem* **266**, 15790–15796.

Tellinghuisen, T. L., Marcotrigiano, J. & Rice, C. M. (2005). Structure of the zinc-binding domain of an essential component of the hepatitis C virus replicase. *Nature* **435**, 374–379.

Tsuchida, S., Yanagi, S., Inatome, R., Ding, J., Hermann, P., Tsujimura, T., Matsui, T. & Yamamura, H. (2000). Purification of a 72-kDa protein-tyrosine kinase from rat liver and its identification as Syk: involvement of Syk in signaling events of hepatocytes. *J Biochem* **127**, 321–327.

Turner, M., Mee, P. J., Costello, P. S., Williams, O., Price, A. A., Duddy, L. P., Furlong, M. T., Geahlen, R. L. & Tybulewicz, V. L. (1995). Perinatal lethality and blocked B-cell development in mice lacking the tyrosine kinase Syk. *Nature* **378**, 298–302.

Turner, M., Schweighoffer, E., Colucci, F., Di Santo, J. P. & Tybulewicz, V. L. (2000). Tyrosine kinase SYK: essential functions for immunoreceptor signalling. *Immunol Today* **21**, 148–154.

Ulanova, M., Puttagunta, L., Marcet-Palacios, M., Duszyk, M., Steinhoff, U., Duta, F., Kim, M. K., Indik, Z. K., Schreiber, A. D. & Befus, A. D. (2005). Syk tyrosine kinase participates in β1-integrin signaling and inflammatory responses in airway epithelial cells. *Am J Physiol Lung Cell Mol Physiol* **288**, L497–L507.

Wang, S., Ding, Y. B., Chen, G. Y., Xia, J. G. & Wu, Z. Y. (2004). Hypermethylation of Syk gene in promoter region associated with oncogenesis and metastasis of gastric carcinoma. *World J Gastroenterol* **10**, 1815–1818.

Weiss, A. & Littman, D. R. (1994). Signal transduction by lymphocyte antigen receptors. *Cell* **76**, 263–274.

Wienands, J., Larbolette, O. & Reth, M. (1996). Evidence for a preformed transducer complex organized by the B cell antigen receptor. *Proc Natl Acad Sci U S A* **93**, 7865–7870.

Yamada, T., Fujieda, S., Yanagi, S., Yamamura, H., Inatome, R., Sunaga, H. & Saito, H. (2001). Protein-tyrosine kinase Syk expressed in human nasal fibroblasts and its effect on RANTES production. *J Immunol* **166**, 538–543.

Yanagi, S., Kurosaki, T. & Yamamura, H. (1995). The structure and function of nonreceptor tyrosine kinase $p72^{SYK}$ expressed in hematopoietic cells. *Cell Signal* **7**, 185–193.

Yanagi, S., Inatome, R., Ding, J., Kitaguchi, H., Tybulewicz, V. L. & Yamamura, H. (2001). Syk expression in endothelial cells and their morphologic defects in embryonic Syk-deficient mice. *Blood* **98**, 2869–2871.

Yasui, K., Wakita, T., Tsukiyama-Kohara, K., Funahashi, S. I., Ichikawa, M., Kajita, T., Moradpour, D., Wands, J. R. & Kohara, M. (1998). The native form and maturation process of hepatitis C virus core protein. *J Virol* **72**, 6048–6055.

Yuan, Y., Mendez, R., Sahin, A. & Dai, J. L. (2001). Hypermethylation leads to silencing of the *SYK* gene in human breast cancer. *Cancer Res* **61**, 5558–5561.

Yuan, Y., Wang, J., Li, M., Yan, Z., Zhang, C. & Dai, J. L. (2006). Frequent epigenetic inactivation of spleen tyrosine kinase gene in human hepatocellular carcinoma. *Clin Cancer Res* **12**, 6687–6695.

Zech, B., Kurtenbach, A., Krieger, N., Strand, D., Blencke, S., Morbitzer, M., Salassidis, K., Cotten, M., Wissing, J. & other authors (2003). Identification and characterization of amphiphysin II as a novel cellular interaction partner of the hepatitis C virus NS5A protein. *J Gen Virol* **84**, 555–560.

Zhang, J., Berenstein, E. & Siraganian, R. P. (2002). Phosphorylation of Tyr342 in the linker region of Syk is critical for Fc-εRI signaling in mast cells. *Mol Cell Biol* **22**, 8144–8154.

Journal of General Virology (2006), 87, 1935–1945 DOI 10.1099/vir.0.81701-0

Non-structural protein 4A of *Hepatitis C virus* accumulates on mitochondria and renders the cells prone to undergoing mitochondria-mediated apoptosis

Yuki Nomura-Takigawa,[1] Motoko Nagano-Fujii,[1] Lin Deng,[1] Sohei Kitazawa,[2] Satoshi Ishido,[1]† Kiyonao Sada[1] and Hak Hotta[1]

Correspondence
Hak Hotta
hotta@kobe-u.ac.jp

Divisions of Microbiology[1] and Molecular Pathology[2], Kobe University Graduate School of Medicine, 7-5-1 Kusunoki-cho, Chuo-ku, Kobe 650-0017, Japan

Non-structural protein 4A (NS4A) of *Hepatitis C virus* (HCV) functions as a cofactor for NS3 by forming a complex with it to augment its enzymic activities. NS4A also forms a complex with other HCV proteins, such as NS4B/NS5A, to facilitate the formation of the viral RNA replication complex on the endoplasmic reticulum (ER) membrane. In addition to its essential role in HCV replication, NS4A is thought to be involved in viral pathogenesis by affecting cellular functions. In this study, it was demonstrated that NS4A was localized not only on the ER, but also on mitochondria when expressed either alone or together with NS3 in the form of the NS3/4A polyprotein and in the context of HCV RNA replication in Huh7 cells harbouring an HCV RNA replicon. Moreover, NS4A expression altered the intracellular distribution of mitochondria significantly and caused mitochondrial damage, as evidenced by the collapsed mitochondrial transmembrane potential and release of cytochrome *c* into the cytoplasm, which led ultimately to induction of apoptosis through activation of caspase-3, but not caspase-8. Consistently, Huh7 cells expressing NS3/4A and those harbouring an HCV RNA replicon were shown to be more prone to undergoing actinomycin D-induced, mitochondria-mediated apoptosis, compared with the control Huh7 cells. Taken together, these results suggest the possibility that HCV exerts cytopathic effect (CPE) on the infected cells under certain conditions and that NS4A is responsible, at least in part, for the conditional CPE in HCV-infected cells.

Received 19 November 2005
Accepted 22 February 2006

INTRODUCTION

Hepatitis C virus (HCV), a member of the family *Flaviviridae*, has a single-stranded, positive-sense RNA of about 9·6 kb in length. The virus genome encodes a precursor polyprotein of about 3000 aa, which is cleaved into at least 10 mature viral proteins, such as Core, E1, E2, p7, NS2, NS3, NS4A, NS4B, NS5A and NS5B (Reed & Rice, 2000). HCV is known to evade the host-defence mechanisms to establish persistent infection, causing chronic hepatitis, liver cirrhosis and hepatocellular carcinoma (Kiyosawa *et al.*, 1990; Tong *et al.*, 1995). It has been suggested that liver-cell injuries, either apoptotic or necrotic changes, are mediated principally by antiviral immune responses, such as HCV-specific cytotoxic T lymphocytes. However, the possible involvement of viral cytopathic effect (CPE) should also be taken into consideration.

Apoptosis involves two major pathways: the Fas-mediated pathway and the mitochondria-mediated pathway (Ashkenazi & Dixit, 1998; Gewies *et al.*, 2000). Fas-mediated apoptosis is conducted through facilitation of caspase-8 activation. Regarding HCV infection, Core was shown to induce Fas-mediated and tumour necrosis factor (TNF) receptor-mediated apoptosis (Ruggieri *et al.*, 1997). On the other hand, a number of apoptosis-inducing signals are concentrated at mitochondria to facilitate the release of cytochrome *c* from mitochondria, which induces formation of an apoptosome complex that includes apoptosis protease-activating factor-1 (Apaf-1) and procaspase-9 (Deveraux *et al.*, 1998; Fearnhead *et al.*, 1998; Gross *et al.*, 1999; Skulachev, 1998). This results in the activation of caspases and finally the cleavage of chromosomal DNA. Thus, mitochondria are intensive and central organelles regulating apoptotic signals.

A wide variety of viral proteins have been shown to localize specifically on mitochondria, such as cytomegalovirus vMIA (Goldmacher *et al.*, 1999), myxoma virus M11L (Everett *et al.*, 2002), Kaposi's sarcoma-associated herpesvirus K7 (Feng *et al.*, 2002; Wang *et al.*, 2002), human

†Present address: Laboratory for Infectious Immunity, RIKEN Research Center for Allergy and Immunology, 1-7-22 Suehiro-cho, Tsurumi-ku, Yokohama, Kanagawa 230-0045, Japan.

immunodeficiency virus type 1 Vpr (Jacotot *et al.*, 2000, 2001), human T-cell leukemia virus type 1 $p13^{II}$ (D'Agostino *et al.*, 2002), influenza virus PB1-F2 (Chen *et al.*, 2001), hepatitis B virus X protein (Rahmani *et al.*, 2000) and HCV Core (Schwer *et al.*, 2004). Some of them exert anti-apoptotic effects, and the others pro-apoptotic ones, by binding to apoptosis-regulating host-cell factors.

HCV NS4A is a non-structural protein of about 7 kDa that consists of 54 aa with a hydrophobic N-terminal region and a hydrophilic C terminus. NS4A is known to function as a cofactor for NS3 to augment its enzymic activities, such as serine protease (Failla *et al.*, 1995; Reed & Rice, 2000; Satoh *et al.*, 1995) and RNA and DNA helicases (Kuang *et al.*, 2004; Pang *et al.*, 2002; Reed & Rice, 2000). NS3 and NS4A, together with the other non-structural proteins, are incorporated into the HCV RNA replication complex, which is localized primarily on the endoplasmic reticulum (ER) and related membrane structures (Aizaki *et al.*, 2004; Egger *et al.*, 2002; Gosert *et al.*, 2003; Kim *et al.*, 1999; Wölk *et al.*, 2000). Little is known, however, about the possible effect(s) of NS4A on cellular functions, except for a few studies, including ours, showing that NS4A markedly inhibits the translation of the host cell (Florese *et al.*, 2002; Kato *et al.*, 2002).

In this study, we report that NS4A is localized not only on the ER, but also on mitochondria, and that NS4A induces apoptosis through a mitochondria-mediated pathway, as demonstrated by the decreased mitochondrial transmembrane potential, the release of cytochrome *c* from mitochondria and the activation of caspase-3, followed by the morphological changes characteristic of apoptotic cell death. We have also observed that Huh7 cells harbouring an HCV subgenomic RNA replicon are more prone to apoptosis than are control cells when treated with mitochondria-mediated apoptosis-inducing reagents, such as actinomycin D and staurosporine. These results collectively suggest the possibility that NS4A is one of the viral factors that induces CPE under certain conditions.

METHODS

Construction of expression plasmids. A cDNA fragment encoding the full-length NS4A of HCV subtype 1b (Con1 strain) was amplified by PCR from pFK5B2884Gly (a kind gift from Dr R. Bartenschlager, University of Heidelberg, Heidelberg, Germany) (Lohmann *et al.*, 2001). The amplified fragment was digested with *Eco*RI and subcloned into the unique *Eco*RI site of pSG5 (Stratagene) to generate pSG5-NS4A. Plasmids to express FLAG-tagged full-length NS4A and a C-terminally deleted mutant were constructed as reported previously with minor modifications (Florese *et al.*, 2002; Taguchi *et al.*, 2004). Other pSG5-based expression plasmids, such as pSG5-Core, -NS3, -NS4B, -NS3/4A, -NS5A and -NS5B, were described elsewhere (Deng *et al.*, 2006; Florese *et al.*, 2002; Ishido *et al.*, 2000; Song *et al.*, 1999; Wang *et al.*, 2000).

Cell culture and transfection. Huh7 cell lines harbouring an HCV subgenomic RNA replicon (Huh7-FK2884Gly-1 cells) that expresses NS3 to NS5B were reported previously (Lohmann *et al.*, 2001; Taguchi *et al.*, 2004; Takigawa *et al.*, 2004). The parental Huh7 cells served as a control. For transient expression of each HCV protein, Huh7 cells were transfected with an expression plasmid by using FuGENE 6 transfection reagent (Roche Diagnostics).

Cell-viability assay. Cells were seeded in 96-well plastic plates. Cell viability was determined based on mitochondrial NADH-dependent dehydrogenase activity by WST-1 assay using a sulfonated tetrazolium salt, 2-(4-iodophenyl)-3-(4-nitrophenyl)-5-(2,4-disulfophenyl)-2H-tetrazolium monosodium salt, as reported previously (Fujita *et al.*, 1996; Ishido *et al.*, 2000). A_{450} was read with a microplate photometer (Bio-Rad). Octuplicate cultures were prepared for each sample and the results were presented as a percentage of the value for untreated controls.

Subcellular fractionation. Cells (1×10^7) were harvested with a cell scraper and the cell suspension was centrifuged at 200 *g* for 5 min at 4 °C. The cells were resuspended in an ice-cold homogenization buffer containing 100 mM Tris/HCl (pH 8·0), 250 mM sucrose, 2 mM EDTA and protease inhibitors (Complete; Roche Molecular Biochemicals) and homogenized by using a homogenizer by 30 strokes at speed 4·4 of a motor-driven pestle (Wheaton overhead stirrer). The homogenate was centrifuged at 900 *g* for 10 min at 4 °C twice. Subsequently, the supernatant, deprived of the nuclei and unbroken cells, was centrifuged at 10 000 *g* for 10 min at 4 °C to collect mitochondria. The supernatant was further centrifuged at 100 000 *g* for 1 h and the pellet containing the ER was obtained. Each subcellular fraction was determined by immunoblotting with antibodies against protein disulfide isomerase (PDI) (Becton Dickinson) and mtHSP70 (Affinity BioReagents, Inc.) as markers for ER and mitochondria, respectively.

Immunoblotting. Cell lysates in a buffer containing 50 mM Tris/HCl (pH 6·8), 2 % SDS, 10 % glycerol and bromophenol blue were electrophoresed on 14–16 % SDS-polyacrylamide gels and transferred to nitrocellulose membranes as described previously (Muramatsu *et al.*, 1997). After being blocked with skimmed milk for 1 h at room temperature followed by washing with PBS containing 0·05 % Tween 20 (PBS-T), the membrane was incubated with an appropriate first antibody for 1 h, washed three times with PBS-T and incubated with a peroxidase-labelled second antibody at room temperature for 30 min. After being washed three times with PBS-T, the positive bands were visualized by using the ECL detection system (Amersham Biosciences) according to the manufacturer's instructions.

Immunofluorescence microscopy. Cells were fixed with 3·7 % formaldehyde for 10 min at room temperature and permeabilized with 0·1 % Triton X-100 for 10 min at room temperature. After being washed with PBS, the cells were incubated with a first antibody for 1 h, followed by washing three times with PBS-T and staining with a fluorescein isothiocyanate (FITC)-, Cy3- or Alexa Fluor 546-labelled second antibody. The first antibodies used were mouse mAbs against Core, NS3, NS4A and NS5A (kind gifts from Dr I. Yoshida, Research Institute for Microbial Diseases, Osaka University, Kan-Onji branch, Kagawa, Japan). The cells were washed again with PBS-T, mounted with 80 % glycerol and observed under a fluorescence microscope (Olympus) or a confocal immunofluorescence microscope (Carl Zeiss). MitoTracker (Molecular Probes) and pEYFP-Golgi (Clontech) were used for staining mitochondria and the Golgi apparatus, respectively.

Immunoelectron microscopy. Immunoelectron microscopy was performed as described previously with some modifications (Hidajat *et al.*, 2005). In brief, cells were fixed with 4 % paraformaldehyde and 1 % glutaraldehyde in 150 mM HEPES-KOH (pH 7·4) for 10 min at room temperature. The cells were collected by a cell scraper, centrifuged and dehydrated through a series of 50, 70, 80, 90 and 100 % ethanol. The sample was embedded in LR White resin (London Resin Co. Ltd) and kept at −20 °C for 2 days. After ultrathin

sectioning, sections were blocked with 0·5 % BSA solution and incubated with anti-NS4A mouse mAb for 1 h at room temperature. After being washed with PBS, the sections were incubated with goat anti-mouse IgG conjugated to 10 nm gold (Sigma) for 30 min at room temperature. After being washed with PBS and extra-pure water, the sections were dried, stained with lead citrate and observed under an electron microscope (JEM-1200EX; JOEL).

Mitochondrial transmembrane potential. Changes in the mitochondrial transmembrane potential were examined by using rhodamine 123 (Rho123; Sigma). Rho123, a fluorescent, lipophilic, cationic dye, accumulates in mitochondria of living cells and has been used for evaluating changes in the mitochondrial transmembrane potential (Davis *et al.*, 1985; Leprat *et al.*, 1990; Li *et al.*, 1999; Lin *et al.*, 2004). Cells (5×10^5) were washed with PBS and stained with a staining solution containing Rho123 (0·5 μg ml^{-1}) for 15 min at 37 °C. The fluorescence emitted from Rho123 was analysed by a flow cytometer (Becton Dickinson).

Caspase enzymic activity. Caspase-3 activity was measured by using Caspase-GloTM 3/7 reagent (Promega) according to the manufacturer's instructions. In brief, a proluminescent caspase-3/7 substrate, which contains the tetrapeptide sequence DEVD, was added to cells cultured on a microplate. The cells were incubated for 30 min at room temperature and the luminescence of each sample was measured by a microplate luminometer (Luminescencer-JNP AB-2100; ATTO). Caspase-8 activity was measured by using a FLICE/Caspase-8 colorimetric protease assay kit (Medical Biological Laboratories Co. Ltd) according to the manufacturer's instructions. Cells were detached from the dishes with trypsin and lysed in an ice-cold lysis buffer supplied with the kit for 10 min. The cytosolic extracts obtained were mixed with IETD-*p*NA, the substrate of caspase-8, and incubated for 2 h at 37 °C. A_{405} was read with a microplate photometer (Bio-Rad).

Cytological markers for apoptosis: morphological changes of the nuclei. Cells were fixed with 100 % methanol at −20 °C for 20 min, washed twice with PBS and stained with 10 μM Hoechst 33342 at room temperature for 10 min, as described previously (Fujita *et al.*, 1996; Ishido *et al.*, 2000). The morphology of the nuclei of the cells was examined under a light microscope.

RESULTS

NS4A is localized on mitochondria

We first examined the intracellular localization of NS4A. Immunofluorescence analysis revealed that NS4A colocalized with MitoTracker, a marker for mitochondria, in Huh7 cells using a transient-expression system (Fig. 1a, top). It should be noted that, in NS4A-expressing cells, mitochondria accumulated in the perinuclear region, exhibiting a doughnut-like appearance. NS4A was also localized at the ER to a considerable degree (Fig. 1a, middle) and, to a much lesser degree, at the Golgi apparatus (bottom). Mitochondrial localization of NS4A was observed when NS4A was co-expressed with NS3 *in cis* as well (Fig. 1b, top). We also tested the possible mitochondrial localization of the other HCV proteins, such as Core, NS3, NS4B and NS5A, and found that Core and NS5A were partially localized on mitochondria. Unlike NS4A, however, none of these HCV proteins altered the intracellular-distribution pattern of mitochondria. The mitochondrial localization of NS4A in Huh7 cells was confirmed by further experiments. Subcellular-fractionation analysis revealed that NS4A was detected abundantly in a mitochondrial fraction of Huh7 cells in a transient-expression system (Fig. 1c). Moreover, NS4A was detected in a mitochondrial fraction obtained from Huh7 cells harbouring an HCV subgenomic RNA replicon. PDI, an ER marker, was barely detected, if at all, in the mitochondrial fraction, with the result excluding the possible contamination of the mitochondrial fraction with the ER and thereby verifying the specificity of the mitochondrial localization of NS4A in those cells. Confocal immunofluorescence microscopic analysis revealed that NS4A was partially colocalized on mitochondria in Huh7 cells harbouring the HCV subgenomic RNA replicon, although to a lesser extent than that observed in cells expressing NS4A or NS3/4A transiently (Fig. 1d). Also, immunoelectron microscopic analysis demonstrated clearly that NS4A was localized on both ER and mitochondria of Huh7 cells expressing NS4A transiently (Fig. 1e) and those harbouring the HCV RNA replicon (Fig. 1f). The immunogold staining was not observed in the control cells without NS4A expression, ensuring the specificity of the staining (data not shown). From these results, we concluded that NS4A was localized preferentially on mitochondria. We also speculated that NS4A could potentially alter the intracellular distribution and functions of mitochondria.

NS4A induces cell death

While analysing the intracellular localization of NS4A, we noticed that NS4A-expressing cells exhibited severe cell damage after prolonged cultivation. In line with this observation, we could not generate any Huh7 cell line stably expressing NS4A (data not shown). We therefore examined the possible effect of NS4A on cell viability. The result demonstrated that NS4A caused cell death (Fig. 2). When NS4A was co-expressed with NS3 *in cis* (NS3/4A), cell death was not observed, although a comparable level of NS4A expression was achieved in these cells. These results suggest that, under these experimental conditions, the cell death-inducing effect of NS4A was abolished after forming a complex with NS3. This result, however, does not necessarily exclude the possibility that NS3/4A could affect cell death under certain conditions (see below).

NS4A induces the collapse of the mitochondrial transmembrane potential

To assess the molecular mechanism of NS4A-induced cell death, we first measured the mitochondrial transmembrane potential by using Rho123. In this analysis, Huh7 cells transiently transfected with the pSG5 vector and those treated with staurosporine served as a negative and a positive control, respectively. As shown in Fig. 3, a larger number of NS4A-expressing cells showed decreased mitochondrial transmembrane potential (24·0 %) compared with the non-expressing control (7·6 %) and cells expressing NS3 alone (10·5 %). Again, the mitochondria-damaging effect of NS4A was counteracted by NS3 (NS3/4A; 9·5 %).

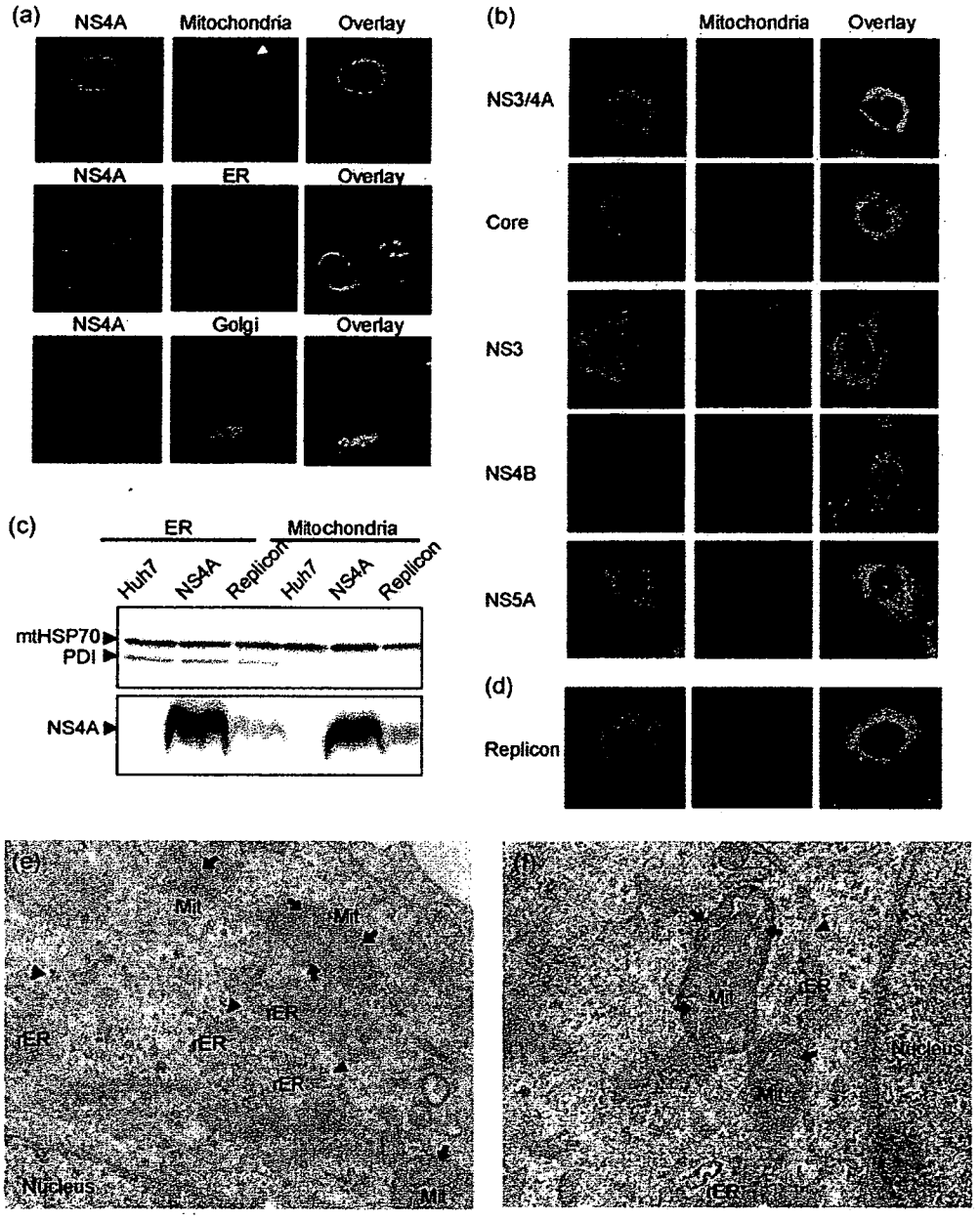

Fig. 1. Localization of NS4A on mitochondria. (a) Immunofluorescence analysis. Huh7 cells expressing NS4A transiently were double-stained with anti-NS4A mouse mAb (left panels) and MitoTracker Red (upper middle panel), anti-calregulin rabbit antiserum as an ER marker (centre) or pEYFP-Golgi (lower middle panel). Second antibodies used were either FITC-conjugated anti-mouse IgG (green), Cy3-conjugated anti-rabbit IgG (red) or Alexa Fluor 546-conjugated anti-mouse IgG (red). Overlaid pictures are shown on the right. Note a doughnut-like, perinuclear staining of mitochondria in NS4A-expressing cells (upper middle panel, arrowhead). (b) Huh7 cells transiently expressing NS3/4A were stained with anti-NS4A antibody plus FITC-conjugated anti-mouse IgG (left panel) and MitoTracker Red as a mitochondrial marker (centre). Also, cells expressing Core, NS3, NS4B and NS5A transiently were double-stained with specific antibodies (Core, NS3 and NS5A) or HCV-infected patient serum (NS4B) and MitoTracker Red. Second antibodies used were FITC-conjugated anti-mouse IgG or anti-human IgG. Overlaid pictures are shown on the right. (c) Subcellular fractionation. Huh7 cells expressing NS4A transiently, those harbouring an HCV subgenomic RNA replicon and the parental control were fractionated. The ER and mitochondrial fractions were probed with anti-NS4A antibody. The absence of ER in the mitochondrial fraction was confirmed by staining with antibodies against PDI. (d) Huh7 cells harbouring an HCV subgenomic RNA replicon were stained with anti-NS4A antibody plus FITC-conjugated anti-mouse IgG (left panel) and MitoTracker Red (centre). An overlaid picture is shown on the right. (e) Immunoelectron microscopic analysis of Huh7 cells expressing NS4A transiently. Arrows and arrowheads indicate NS4A localized at mitochondria and ER, respectively. (f) Immunoelectron microscopic analysis of Huh7 cells harbouring an HCV subgenomic RNA replicon. Arrows and arrowheads indicate NS4A localized at mitochondria and ER, respectively. Mit, Mitochondrion; rER, rough ER.

NS4A induces the release of cytochrome c from mitochondria

The collapse of the mitochondrial transmembrane potential would impair the intrinsic functions of mitochondria, triggering apoptosis and/or necrosis. Cytochrome *c* is normally present in the mitochondrial intermembrane space and is released to the cytosol when cells undergo apoptosis. We therefore examined whether expression of NS4A could trigger the release of cytochrome *c* from mitochondria. As had been expected, nearly 70% of NS4A-expressing Huh7 cells, but not the empty vector-transfected control, showed the release of cytochrome *c* into the cytoplasm 48 h after transfection, as evidenced by diffuse staining of cytochrome *c* throughout the cell (Fig. 4a, b). Expression of Core (Fig. 4b), NS4B and NS5A (data not shown), but not NS3, each induced cytochrome *c* release only slightly (~10%). Cells expressing NS3/4A did not induce cytochrome *c* release, but rather exhibited doughnut-like, perinuclear staining of cytochrome *c* (Fig. 4a, b). The absence of cytochrome *c* release in NS3/4A-expressing cells was confirmed even 96 h after transfection (data not shown). The doughnut-like staining pattern of NS4A closely resembled that of mitochondrial localization in cells expressing either NS4A alone or NS3/4A (Fig. 1a, b). These results collectively suggest the possibility that both NS4A by itself and the NS3/4A complex accumulate on mitochondria, but that they exert differential effects on the cellular conditions depending upon its molecular status.

Cytochrome *c* release was observed in cells expressing NS4AΔC14 (Fig. 4b). A comparable expression level of full-length NS4A and NS4AΔC14 was verified by immunoblotting. These results suggested that the C-terminal 14 residues of NS4A were not involved in the induction of cytochrome *c* release.

NS4A activates caspase-3, but not caspase-8, and induces apoptosis

Cytochrome *c*, once released to the cytosol, plays an important role in the activation of caspase-3, which is a principal effector for induction of apoptosis (Liu *et al.*, 1996). Consistent with this idea, we observed that caspase-3 activity was enhanced in NS4A-expressing Huh7 cells compared with the non-expressing control (Fig. 5a, left panel). On the other hand, caspase-8 was not activated by NS4A expression (Fig. 5a, right panel). Caspase-8 is known to be involved in the Fas-mediated apoptotic pathway (Muzio *et al.*, 1996; Shu *et al.*, 1997). NS4A-mediated cell death was inhibited almost completely by treatment with Z-VAD-fmk, a general inhibitor of caspases (Fig. 5b). These results collectively suggested that NS4A induced apoptosis through the mitochondria-mediated, but not the Fas-mediated, pathway.

To confirm that the NS4A-mediated cell death was due to apoptosis, the nuclei of the cells were stained with Hoechst 33342 and their morphology was examined. Chromatin condensation and nuclear fragmentation, typical cytological markers for apoptosis, were observed in NS4A-expressing cells as well as in staurosporine-treated, positive-control cells (Fig. 6a). A similar morphological change of the nucleus was also observed in NS3/4A-expressing cells more frequently than in the vector-transfected control (Fig. 6b). This result implies the possibility that the NS3/4A complex exerts certain effects on cell function, but that the possible effect on cell survival may not become evident in the absence of additional factor(s).

NS3/4A-expressing Huh7 cells are prone to undergoing mitochondria-mediated apoptosis

We hypothesized that the NS3/4A complex might direct the cells to a pre-apoptotic status that, upon exposure to an otherwise ineffective low dose of apoptotic stimuli, leads the cells to apoptosis. To examine this possibility, cells expressing NS3/4A or NS4A alone and the non-expressing control were treated with a suboptimal dose of actinomycin D (100 ng ml^{-1}) and cell viability was determined. The results obtained revealed that NS3/4A-expressing cells, as well as those expressing NS4A alone, were more prone to undergoing actinomycin D-induced (mitochondria-mediated)

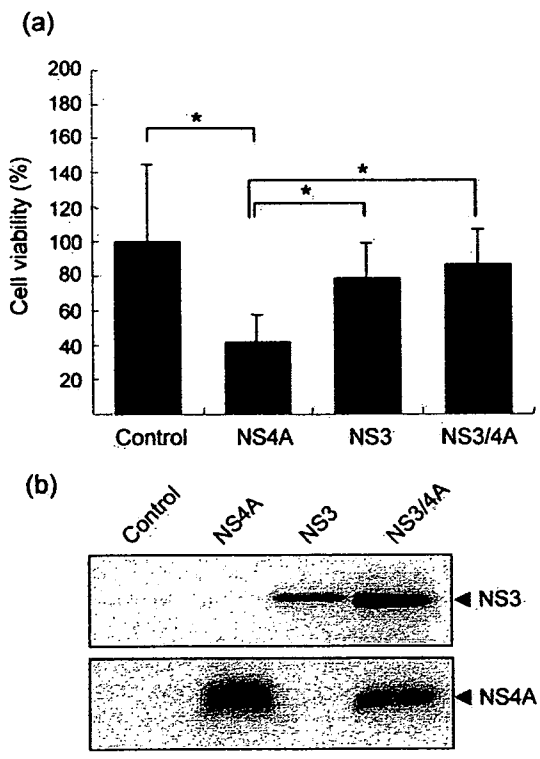

Fig. 2. (a) Cell death induced by NS4A. Huh7 cells expressing NS4A, NS3 and NS3/4A transiently for 48 h, as well as a vector-transfected, non-expressing control, were examined for cell viability by WST-1 assay. Cell viability of plasmid-harbouring cells was calculated. *$P<0.01$ (Student's *t*-test). (b) Expression levels of NS3 and NS4A were determined by immunoblotting (bottom).

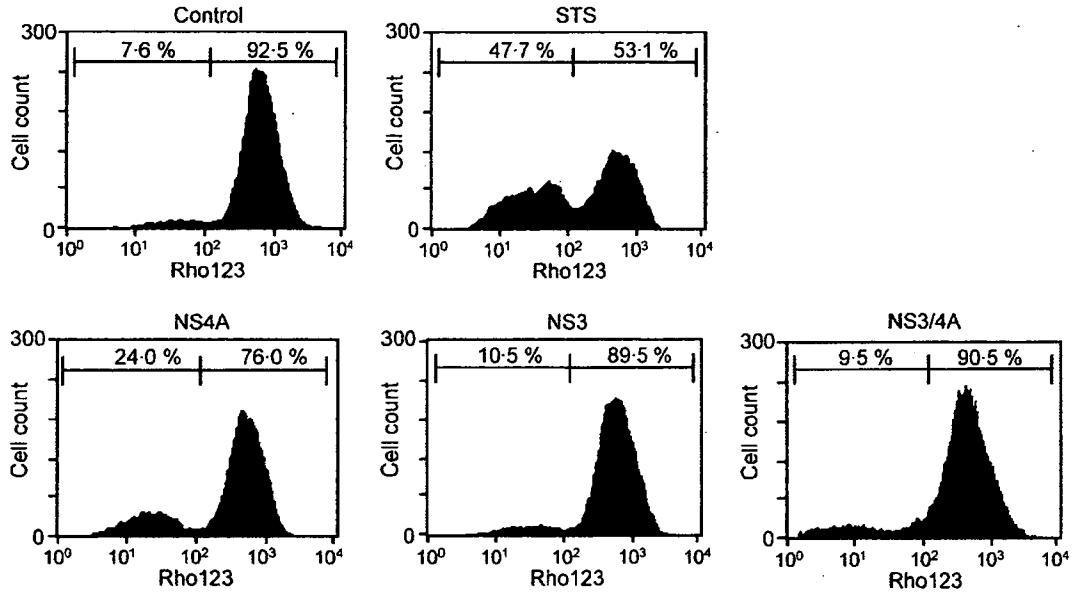

Fig. 3. Collapse of the mitochondrial transmembrane potential by NS4A. Huh7 cells expressing NS4A, NS3 and NS3/4A for 24 h transiently, as well as a vector-transfected, non-expressing control, were measured for the mitochondrial transmembrane potential by staining the cells with Rho123 followed by flow-cytometric analysis. Cells treated with staurosporine (STS, 1 μM) for 6 h served as a positive control. Reduced Rho123 staining indicates the mitochondrial transmembrane potential reduction.

apoptosis than the control cells (Fig. 6c). Similar results were obtained when the cells were treated with 50 ng actinomycin D ml^{-1} (data not shown).

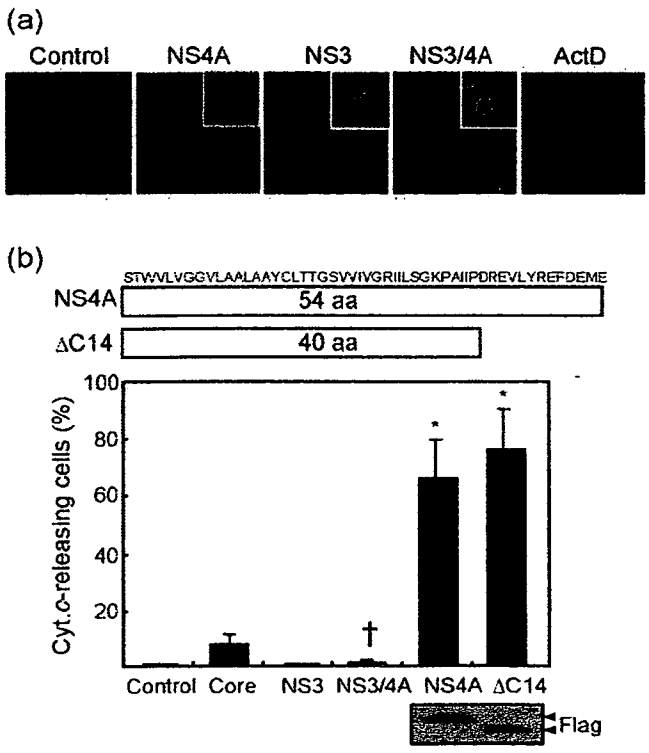

Fig. 4. Cytochrome *c* release from mitochondria into the cytoplasm by NS4A. (a) Huh7 cells expressing NS4A, NS3 and NS3/4A transiently for 48 h, as well as the vector-transfected, non-expressing control, were stained with anti-cytochrome *c* mouse mAb and Alexa Fluor 546-conjugated anti-mouse IgG. Expression of NS4A and NS3 was confirmed by staining the cells with HCV-infected patient serum that reacted strongly to NS4A and NS3, followed by FITC-conjugated anti-human IgG (right upper corner of the three panels). Cells treated with actinomycin D (ActD; 300 ng ml^{-1}) for 24 h served as a positive control. (b) Percentage of cells showing cytochrome *c* release among plasmid-harbouring cells. Huh7 cells expressing Core, NS3, NS3/4A, FLAG-tagged NS4A and FLAG-tagged NS4AΔC14 transiently, as well as the vector-transfected, non-expressing control, were tested. *$P<0{\cdot}01$ compared with the control (Student's *t*-test). †All of the NS3/4A-expressing cells showed perinuclear accumulation of cytochrome *c* staining (see Fig. 4a), which coincided with the mitochondrial-localization pattern, as evidenced by staining with a mitochondrial marker (MitoTracker). An equivalent expression level of FLAG-tagged NS4A and FLAG-tagged NS4AΔC14 was verified by immunoblotting (bottom).

Huh7 cells harbouring an HCV subgenomic RNA replicon are prone to undergoing mitochondria-mediated, but not Fas-mediated, apoptosis

In cells infected with HCV or those harbouring an HCV RNA replicon, NS4A is expressed in the context of virus replication, where NS4A is principally incorporated into the viral RNA replication complex together with other

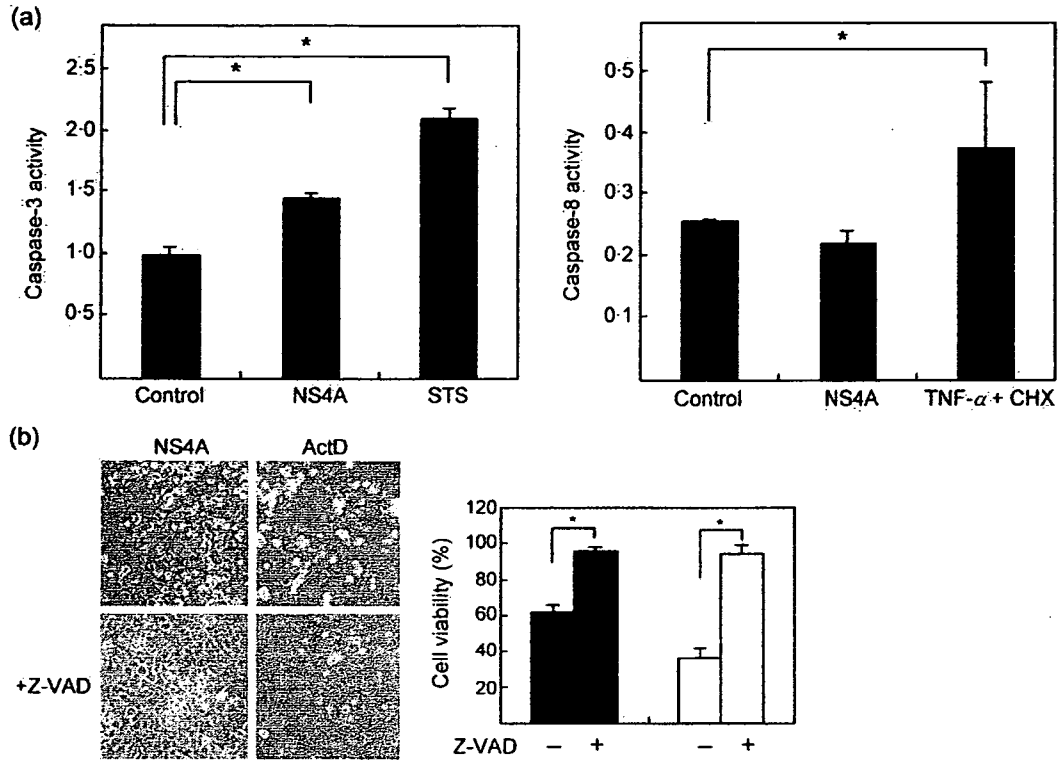

Fig. 5. Activation of caspase-3, but not caspase-8, by NS4A. (a) Huh7 cells expressing NS4A transiently for 24 h and a vector-transfected, non-expressing control were examined for caspase-3 (left panel) and caspase-8 (right panel) activities. Cells treated with staurosporine (STS, 1 μM) for 3 h and those treated with TNF-α (50 ng ml^{-1}) and cycloheximide (CHX, 5 μg ml^{-1}) for 6 h served as positive controls for caspase-3 and caspase-8 measurements, respectively. *$P<0·01$ (Student's *t*-test). (b) Inhibition of NS4A-induced cell death by a caspase inhibitor, Z-VAD-fmk. Huh7 cells expressing NS4A (left panels) and those treated with actinomycin D (ActD; 300 ng ml^{-1}) for 24 h (right panels) were cultured in the absence (upper panels) or presence of 20 μM Z-VAD-fmk (lower panels) and observed under an inverted microscope. Percentage of cell viability among plasmid-transfected cells was calculated and shown on the right (filled bars, NS4A; empty bars, ActD). *$P<0·01$ (Student's *t*-test).

non-structural proteins. We therefore examined whether Huh7 cells harbouring an HCV subgenomic RNA replicon are prone to undergoing apoptosis under some circumstances. As shown in Fig. 7(a), the replicon-harbouring cells underwent actinomycin D-induced (mitochondria-mediated) apoptosis to a significantly larger extent than that observed with the non-expressing control. On the other hand, no difference in the degree of TNF-α-induced apoptosis was observed between the replicon-harbouring cells and the control Huh7 cells. Similar results were obtained reproducibly with two other independent clones harbouring the same HCV RNA replicon (data not shown). The collapse of the mitochondrial transmembrane potential was significantly more evident in the replicon-harbouring cells (35·7%) than in the control (10·0%) when treated with actinomycin D (Fig. 7b).

DISCUSSION

HCV infection in the liver causes apoptotic and/or necrotic cell death of hepatocytes. The cell death is thought to be mediated principally by HCV-specific cytotoxic T cells; however, direct CPE by the virus itself should not be overlooked. Many viruses, including HCV, possess viral proteins that either promote or inhibit cell death. Among HCV proteins, Core (Sacco *et al.*, 2003), NS2 (Erdtmann *et al.*, 2003), NS3 (Fujita *et al.*, 1996) and NS5A (He *et al.*, 2002; Lan *et al.*, 2002) have been reported to possess anti-apoptotic functions. Also, there are reports showing that Core (Hahn *et al.*, 2000; Moorman *et al.*, 2003; Ruggieri *et al.*, 1997, 2003; Soguero *et al.*, 2002; Zhu *et al.*, 2001), E1 (Ciccaglione *et al.*, 2003, 2004), NS3/4A (Hsu *et al.*, 2003), NS5A and NS5B (Siavoshian *et al.*, 2005) function as pro-apoptotic proteins.

NS4A is known to localize in the ER (Mottola *et al.*, 2002; Reed & Rice, 2000). On the other hand, we demonstrate in the present study that NS4A was localized not only in the ER, but also on mitochondria (Fig. 1). Normally, mitochondria take a filamentous form, with a minor fraction exhibiting a micropunctate appearance, and are distributed evenly in the cell. In NS4A-expressing cells, however, mitochondria took

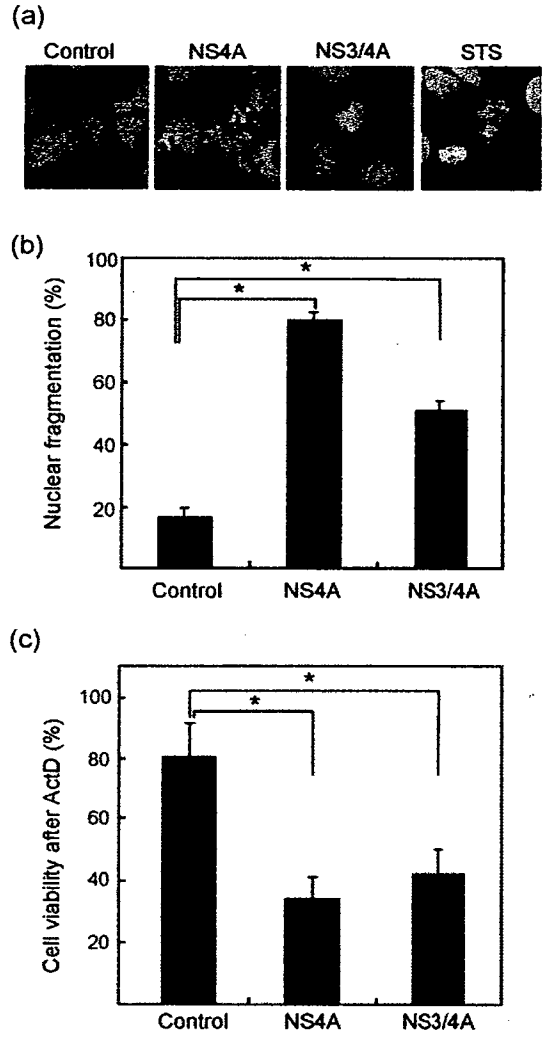

Fig. 6. Evidence for NS4A-induced apoptosis. (a) Huh7 cells expressing NS4A and NS3/4A transiently for 48 h and the vector-transfected, non-expressing control were stained with Hoechst 33342 (10 μM) for 10 min and observed under a fluorescent microscope. Cells treated with staurosporine (STS, 1 μM) for 6 h served as a positive control. (b) Percentage of cells showing nuclear fragmentation was calculated. $^*P<0{\cdot}01$ (Student's *t*-test). (c) Huh7 cells expressing NS4A or NS3/4A transiently and the vector-transfected, non-expressing control were treated with a suboptimal dose of actinomycin D (100 ng ml^{-1}) for 24 h and cell viability was determined.

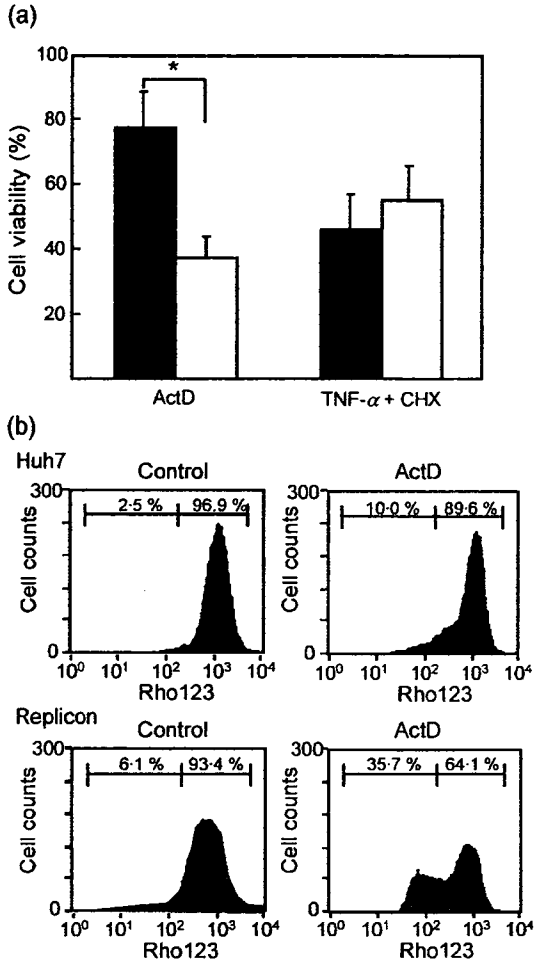

Fig. 7. Increased sensitivity of HCV RNA replicon-harbouring cells to mitochondria-mediated, but not TNF-α-receptor-mediated, apoptotic stimuli. (a) Huh7 cells harbouring an HCV subgenomic RNA replicon (empty bars) and the parental control (filled bars) were left untreated or treated with either actinomycin D (ActD, 100 ng ml^{-1}) for 24 h or TNF-α (50 ng ml^{-1}) and cycloheximide (CHX, 5 μg ml^{-1}) for 9 h. Cell viability was measured by WST-1 assay. $^*P<0{\cdot}01$ (Student's *t*-test). (b) The cells in (a) were analysed for mitochondrial transmembrane potential by using Rho123. Reduced Rho123 staining indicates the mitochondrial transmembrane potential reduction.

a dumpy form and were aggregated in the perinuclear region, exhibiting a doughnut-like appearance (Fig. 1a). Similar perinuclear accumulation of mitochondria was observed also in NS3/4A-expressing cells (Fig. 4a; data not shown). These results suggest the possibility that NS4A, either expressed alone or co-expressed with NS3 so as to form a complex with it, accumulates on mitochondria. The next question that we raised was what would be the consequence of NS4A accumulation on mitochondria. In this regard, we found that NS4A induced mitochondrial transmembrane potential reduction (Fig. 3) and the release of cytochrome *c* into the cytoplasm (Fig. 4). Expression levels of Bax and Bcl-2 were not affected by NS4A or NS3/4A (data not shown), suggesting that a Bax/Bcl-2 imbalance was unlikely to be the cause of the observed mitochondrial damage. The molecular event(s) triggering the mitochondrial damage is/are currently unknown. In any case, cytochrome *c* is usually bound to the inner mitochondrial membrane through an association with the anionic phospholipid cardiolipin. The release of cytochrome *c* from mitochondria triggers the formation of an apoptosome complex that includes Apaf-1, procaspase-9 and ATP, leading to the activation of caspases and eventually apoptosis of the cell. Consistent with this scenario, we

observed NS4A-induced caspase-3 activation (Fig. 5a) and cell death (Fig. 2), the latter of which was blocked by a broad-spectrum caspase inhibitor Z-VAD (Fig. 5b). NS4A-expressing cells exhibited nuclear fragmentation (Fig. 6), which is considered as an apoptosis marker. On the other hand, NS4A did not induce caspase-8 activation (Fig. 5a). It is well-known that caspase-8 is activated upon Fas- and TNF-α-receptor-mediated apoptosis (Muzio *et al.*, 1996; Shu *et al.*, 1997). These results collectively suggest that NS4A induces mitochondria-mediated, but not Fas- or TNF-α-mediated, apoptosis.

NS4A consists of 54 aa, with its N-terminal and central regions being hydrophobic (Failla *et al.*, 1995). Deletion mutational analysis revealed that a C-terminally deleted mutant (NS4AΔC14) also induced the release of cytochrome *c* (Fig. 4b). In this regard, we previously observed that NS4AΔC14 (aa 1–40), but not NS4AΔN17 (aa 18–54) or NS4AΔN17ΔC14 (aa 18–40), inhibited the translation in the cell (Florese *et al.*, 2002). These results imply an important role for the N-terminal hydrophobic region of NS4A in affecting host cellular functions. On the other hand, NS4A is known to bind to NS3 and NS4B/NS5A through its hydrophobic central region. Our results showed that the NS4A-induced apoptosis and reduction in the mitochondrial transmembrane potential were alleviated by NS3 (Figs 2–4). It should be emphasized, however, that the mitochondrial morphology and intracellular localization (Fig. 4a) and the nuclear morphology (Fig. 6a, b) were altered in NS3/4A-expressing cells. This result implies the possibility that the NS3/4A complex, after being transported to mitochondria by virtue of NS4A, exerts a significant effect on mitochondrial function, and possibly even other cellular functions, without affecting mitochondrial transmembrane potential. In fact, we observed that NS3/4A-expressing cells were more sensitive to actinomycin D-induced, mitochondria-mediated apoptosis than the non-expressing control (Fig. 6c). It is not surprising that a virus can mediate mitochondrial dysfunction through a number of different mechanisms. It has recently been reported that NS3/4A cleaves the mitochondrial antiviral signalling protein, MAVS, thereby inhibiting the retinoic acid-inducible gene I-mediated induction of beta interferon production (Li *et al.*, 2005). It is possible that NS3/4A cleaves another mitochondrial protein(s) to modulate mitochondria-mediated cellular activities.

The possible mitochondria-damaging effect of NS4A alone might be weakened in HCV-infected cells, where NS4A is incorporated into the RNA replication complex with NS3, NS4B, NS5A and NS5B. It may explain why HCV RNA replicon-harbouring cells grew well under normal conditions, despite the apoptosis-inducing function of NS4A. Upon receiving a suboptimal degree of apoptotic stimuli, however, Huh7 cells harbouring an HCV subgenomic RNA replicon underwent apoptosis to a larger extent than HCV replicon-free control cells (Fig. 7). This result suggests the possibility that HCV infection renders host cells more sensitive to mitochondria-mediated apoptosis. This notion is in line with previous observations that, in hepatocytes of HCV-infected patients, mitochondria exhibited irregular and dumpy appearances with thin and fragmented cristae (Barbaro *et al.*, 1999) and that hepatocytes of HCV-infected patients underwent apoptosis *in vivo* (Bantel *et al.*, 2001; Bantel & Schulze-Osthoff, 2003; Hayashi *et al.*, 1997; Hiramatsu *et al.*, 1994). HCV-induced apoptosis was also observed in B-cell lymphoma cells *in vitro* (Sung *et al.*, 2003). It should be mentioned that, after receiving a pro-apoptotic stimulus, such as calcium ionophore treatment, cells undergo either apoptosis or necrosis depending upon the amount of ATP available in the microenvironment (Eguchi *et al.*, 1997). Therefore, HCV infection may induce necrosis as well under some conditions. In conclusion, our present data imply the possibility that NS4A is responsible, at least partly, for conditional cell death (CPE) of hepatocytes in HCV-infected patients.

ACKNOWLEDGEMENTS

The authors are grateful to Dr R. Bartenschlager (University of Heidelberg, Heidelberg, Germany) for providing an HCV subgenomic RNA replicon (pFK5B2884Gly). Thanks are also due to Dr I. Yoshida (Research Institute for Microbial Diseases, Osaka University, Kan-Onji Branch, Kagawa, Japan) for providing mouse mAbs against HCV NS3, NS4A and NS5A. This work was supported in part by Grants-in-Aid for Scientific Research from the Ministry of Education, Culture, Sports, Science and Technology, the Japan Society for the Promotion of Science and the Ministry of Health, Labour and Welfare, Japan. This study was also carried out as part of the 21COE Program at Kobe University Graduate School of Medicine.

REFERENCES

Aizaki, H., Lee, K.-J., Sung, V. M.-H., Ishiko, H. & Lai, M. M. C. (2004). Characterization of the hepatitis C virus RNA replication complex associated with lipid rafts. *Virology* **324**, 450–461.

Ashkenazi, A. & Dixit, V. M. (1998). Death receptors: signaling and modulation. *Science* **281**, 1305–1308.

Bantel, H. & Schulze-Osthoff, K. (2003). Apoptosis in hepatitis C virus infection. *Cell Death Differ* **10**, S48–S58.

Bantel, H., Lügering, A., Poremba, C., Lügering, N., Held, J., Domschke, W. & Schulze-Osthoff, K. (2001). Caspase activation correlates with the degree of inflammatory liver injury in chronic hepatitis C virus infection. *Hepatology* **34**, 758–767.

Barbaro, G., Di Lorenzo, G., Asti, A., Ribersani, M., Belloni, G., Grisorio, B., Filice, G. & Barbarini, G. (1999). Hepatocellular mitochondrial alterations in patients with chronic hepatitis C: ultrastructural and biochemical findings. *Am J Gastroenterol* **94**, 2198–2205.

Chen, W., Calvo, P. A., Malide, D. & 10 other authors (2001). A novel influenza A virus mitochondrial protein that induces cell death. *Nat Med* **7**, 1306–1312.

Ciccaglione, A. R., Marcantonio, C., Costantino, A., Equestre, M. & Rapicetta, M. (2003). Expression of HCV E1 protein in baculovirus-infected cells: effects on cell viability and apoptosis induction. *Intervirology* **46**, 121–126.

Ciccaglione, A. R., Marcantonio, C., Tritarelli, E., Equestre, M., Magurano, F., Costantino, A., Nicoletti, L. & Rapicetta, M. (2004).